

THE X^- SOLUTION TO THE ${}^6\text{Li}$ AND ${}^7\text{Li}$ BIG BANG NUCLEOSYNTHESIS PROBLEMS
MOTOHIKO KUSAKABE^{1,2}, TOSHITAKA KAJINO^{1,3}, RICHARD N. BOYD⁴, TAKASHI YOSHIDA
Division of Theoretical Astronomy, National Astronomical Observatory of Japan, Mitaka, Tokyo 181-8588, Japan
kusakabe@th.nao.ac.jp

AND

GRANT J. MATHEWS
Department of Physics and Center for Astrophysics, University of Notre Dame, Notre Dame, IN 46556, USA
Draft version December 1, 2018

ABSTRACT

The ${}^6\text{Li}$ abundance observed in metal poor halo stars appears to exhibit a plateau as a function of metallicity similar to that for ${}^7\text{Li}$, suggesting a big bang origin. However, the inferred primordial abundance of ${}^6\text{Li}$ is ~ 1000 times larger than that predicted by standard big bang nucleosynthesis for the baryon-to-photon ratio inferred from the WMAP data. Also, the inferred ${}^7\text{Li}$ primordial abundance is 3 times smaller than the big bang prediction. We here describe in detail a possible simultaneous solution to both the problems of underproduction of ${}^6\text{Li}$ and overproduction of ${}^7\text{Li}$ in big bang nucleosynthesis. This solution involves a hypothetical massive, negatively-charged leptonic particle that would bind to the light nuclei produced in big bang nucleosynthesis, but would decay long before it could be detected. We consider only the X^- -nuclear reactions and assume that the effect of decay products is negligible, as would be the case if lifetime were large or the mass difference between the charged particle and its daughter were small. An interesting feature of this paradigm is that, because the particle remains bound to the existing nuclei after the cessation of the usual big bang nuclear reactions, a second longer epoch of nucleosynthesis can occur among X^- -nuclei which have reduced Coulomb barriers. The existence of the X^- particles thus extends big bang nucleosynthesis from the first few minutes to roughly five hours. We confirm that reactions in which the hypothetical particle is transferred can occur that greatly enhance the production of ${}^6\text{Li}$ while depleting ${}^7\text{Li}$. We also identify a new reaction that destroys large amounts of ${}^7\text{Be}$, and hence reduces the ultimate ${}^7\text{Li}$ abundance. Thus, big-bang nucleosynthesis in the presence of these hypothetical particles, together with or without an event of stellar processing, can simultaneously solve the two Li abundance problems.

Subject headings: cosmological parameters — dark matter — early universe — elementary particles — nuclear reactions, nucleosynthesis, abundances — stars: Population II

1. INTRODUCTION

A long-standing effort in astrophysics has involved searches for signatures of unstable particles that might have existed in the early Universe, but have long since become extinct. The precision that exists in the abundances of the nuclides produced in big bang nucleosynthesis (BBN) suggests that primordial nucleosynthesis is a good place to look for such signatures. In that context, it is of considerable interest that recent observations (e.g. Asplund et al. 2006) of metal poor halo stars (MPHSs) indicate that the primordial abundances of both ${}^6\text{Li}$ and ${}^7\text{Li}$ may not be in agreement with the predictions of standard BBN. Specifically, the ${}^6\text{Li}$ appears to have an abundance plateau similar to that for ${}^7\text{Li}$ in very low metallicity stars. This suggests a primordial abundance. However the abundance value is roughly a factor of 1000 larger than predicted in standard BBN. A similar, though much less severe, problem exists for ${}^7\text{Li}$ (Ryan et al. 2000; Meléndez & Ramírez 2004; Asplund et al. 2006);

the BBN value that would be consistent with the baryon-to-photon ratio inferred from analysis of the Wilkinson Microwave Anisotropy Probe (WMAP)-power spectrum suggests an abundance that is roughly a factor of three higher than the observed value.

In response to this intriguing ${}^6\text{Li}$ result, a number of solutions have been suggested. Some relate the Li anomalies to the possible existence of unstable heavy particles in the early Universe (Dimopoulos et al. 1988a,b, 1989; Jedamzik 2000; Cyburt et al. 2003; Jedamzik 2004; Kawasaki et al. 2005; Kusakabe et al. 2006) which lead to ${}^6\text{Li}$ production via non-thermal reactions induced by the particle decay. Some have suggested a possible epoch of enhanced cosmic ray nucleosynthesis via the $\alpha + \alpha$ reactions (Rollinde et al. 2006; Prantzos 2006; Kusakabe 2007).

Of interest to the present work, however, is the suggestion in several recent works (Cyburt et al. 2006; Kaplinghat & Rajaraman 2006; Pospelov 2007; Kohri & Takayama 2007; Hamaguchi et al. 2007; Kusakabe et al. 2007; Jedamzik 2008a,b) that heavy negatively charged unstable particles could modify BBN and lead to ${}^6\text{Li}$ production. However, this mechanism would operate in a rather different way from the previous suggestions. In this paradigm, the heavy particles (here denoted as X^-) would bind to the nuclei synthesized during BBN to produce exotic nuclei (hereafter denoted

¹ Department of Astronomy, Graduate School of Science, University of Tokyo, Hongo, Bunkyo-ku, Tokyo 113-0033, Japan

² Research Fellow of the Japan Society for the Promotion of Science

³ Department of Astronomical Science, The Graduate University for Advanced Studies, Mitaka, Tokyo 181-8588, Japan

⁴ Present Address: Lawrence Livermore National Laboratory, 7000 East Avenue, Livermore, CA 94550, USA

as X^- -nuclei). These massive X^- particles would be bound in orbits that would have radii comparable to those of the nuclei to which they were attached. Their presence, however, would reduce the Coulomb barrier seen by incident charged particles, thereby enhancing the thermonuclear reaction rates and allowing a longer duration of BBN in an extended epoch of nucleosynthesis. In the present work we expand upon our previous study (Kusakabe et al. 2007) and describe details of a revised analysis of X^- particle effects on BBN. The focus of the present work is to better quantify the effects of X^- particles on BBN. It is possible, however, that both X^- effects and the X -particle decay contribute to the abundances. In a future work we will consider this, but for now we only address the effects of X^- particles and show that this alone can explain the observed lithium abundances.

In standard BBN, ${}^6\text{Li}$ production is suppressed. It is synthesized primarily via the ${}^4\text{He}(d,\gamma){}^6\text{Li}$ reaction, which has a very small cross section. However, Pospelov (2007) suggested that a large enhancement of the ${}^6\text{Li}$ abundance could result from an X^- bound to ${}^4\text{He}$ (denoted ${}^4\text{He}_X$). This allows for the X^- transfer reaction of ${}^4\text{He}_X(d,X^-){}^6\text{Li}$, which can enhance the production of ${}^6\text{Li}$ by as much as seven orders of magnitude. Subsequently, Hamaguchi et al. (2007) carried out a theoretical calculation of the cross section for this X^- transfer reaction in a quantum three-body model. Their value was about an order of magnitude smaller than that of Pospelov (2007). This difference can be traced to their exact treatment of the quantum tunneling in the fusion process and the use of a better nuclear potential.

In other work, Cyburt et al. (2006) identified the X^- as the supersymmetric counterpart of a tau, i.e., a stau, thereby providing some plausibility for the existence of such particles. They also considered the X^- transfer reactions for ${}^6\text{Li}$, ${}^7\text{Li}$, and ${}^7\text{Be}$ production as Pospelov suggested. Kaplinghat & Rajaraman (2006) observed that the decay of an X^- when bound to ${}^4\text{He}$ occasionally knocks out a proton or neutron to produce ${}^3\text{He}$ or ${}^3\text{H}$, thereby enhancing their abundances in BBN. Those nuclides could then interact with other primordial ${}^4\text{He}$ nuclei at higher energies than those normally associated with the BBN production of ${}^6\text{Li}$. Kohri & Takayama (2007) and Kusakabe et al. (2007) studied the recombination of nuclei with X^- particles, and suggested the possibility that BBN with charged massive particles also destroys ${}^7\text{Li}$ and so solves the ${}^7\text{Li}$ problem as well. In addition, a resonant reaction ${}^7\text{Be}_X(p,\gamma){}^8\text{B}_X$ has recently been proposed (Bird et al. 2007) that further destroys ${}^7\text{Be}_X$ through an atomic excited state of ${}^8\text{B}_X$.

In the present work we have estimated new reaction rates for the X^- transfer reactions suggested by Pospelov (2007) as well as others that could occur. We have reanalyzed the X^- transfer reaction rates estimated in Cyburt et al. (2006) and found them to be negligible based upon the reaction dynamics discussed below.

We have adopted a simple model to estimate the binding energy due to the bound X^- particles for each nucleus involved in BBN. The reaction rates are corrected for the modified nuclear charges and the effective mass resulting from the binding of the X^- particle. The reaction rates, however, are not particularly sensitive to the mass of the X^- particle. Therefore, we have simply

assumed that they are much heavier than the nucleon mass.

In this paper we study the potential consequences of X^- particles on BBN, including recombination of the X^- particles by the existing normal nuclei. Several new reaction processes have been included that can produce or destroy ${}^6\text{Li}$ and ${}^7\text{Li}$ in the early universe. We utilize a fully dynamical description which is solved numerically, and which includes all relevant details of kinetic and chemical equilibrium. The purpose of this present work is to better quantify whether there are observable consequences of the resulting reaction network. The ultimate goal is to better explain the observed overproduction (1000 times) and underproduction (3 times) of the abundances of ${}^6\text{Li}$ and ${}^7\text{Li}$.

In Section 2 we outline some of the details of the calculations we have performed to estimate the thermonuclear reaction rates, and to describe the evolution and abundance of the different nuclei, X^- particles, and X -nuclei during the BBN.

In Section 3, we show the results of BBN with the reactions involving the nuclides that could be formed with the embedded X^- particles. As was done in Jedamzik (2008a), we identify the parameter space for solving both the ${}^6\text{Li}$ and ${}^7\text{Li}$ BBN abundance problems. The present work, however, differs from that of Jedamzik (2008a) in several important ways. Besides differences in some of the relevant reaction rates, there are two major differences. One is the inclusion of X -transfer reactions. Jedamzik (2008a) found that X -transfer reactions involving the charge $Z = 1$ X -nuclei could possibly change the light-element abundances. That result, however, relied on reaction rates which were calculated within the framework of the Born approximation. Recently, however, a detailed study of one of the relevant X -transfer reactions by Hamaguchi et al. (2007) shows that a more realistic calculation gives a much smaller (factor of 10) X -transfer reaction rate. Based upon that study, we conclude that X -transfer reactions can be neglected in this work. Another difference is the assumption that hadronic and electromagnetic (EM) decays are unimportant. That is, we only consider the X -nuclear reactions and assume that the effect of decay products is negligible. This is possible if the decay lifetimes are long and/or the mass difference between the X^- and daughter particle is small. In supersymmetric scenarios for example (e.g. Feng et al. 2003a,b), nearly equal masses would also imply a larger lifetime. Very large lifetimes are ruled out but lifetimes of order a year are very interesting for structure formation (Sigurdson & Kamionkowski 2003).

In Section 4, the effects X^- decay are discussed. Our conclusions are summarized in Section 5.

2. MODEL

In order to perform the nucleosynthesis calculations, we have added the relevant X -nuclei and their reactions to the BBN network code (Kawano 1992). The X -nucleus ${}^4\text{He}_X$ is particularly important for the present work, although the other X -nuclei are included and can significantly affect the results. Both proton and neutron captures involving the X^- particles were included when energetically allowed, as were "transfer reactions." We modified most of the thermonuclear reaction rates on the X -nuclei from the original rates (without X -nuclei). The

two dominant effects were the lowered Coulomb barriers resulting from the X^- in the nucleus, and the modified reduced mass. However, as noted below, there are a number of reactions for which careful additional consideration is required in order to estimate reliable reaction rates.

2.1. Properties of the X^- Particle

The X^- particle is assumed to be leptonic, since there is motivation from particle physics for the existence of such a particle (Cyburt et al. 2006). Identifying these particles as the supersymmetric partners of normal leptons implies that they would also be leptonic but of spin 0. Such sleptonic X^- particles will be initially produced in pairs with X^+ particles. Ultimately, their annihilations in the early universe will freezeout. The final required BBN abundance of the residual X^+X^- pairs will then constrain their annihilation cross section. We show below that this cross section is consistent with a weakly interacting sleptonic particle. We note, that the X^+ particles, though also present during BBN will have negligible interactions with ambient nuclei (compared to X^- particles) due to their Coulomb repulsion and low associated reaction rate. Hence, they can be neglected in the present analysis. It is possible, however, that they could affect the final results to the production of electromagnetic and/or hadronic showers when they decay. That complication will be addressed in a future paper. The focus of the present work, however, is only the effects of X^- particles on BBN.

Ultimately, the product of the X^- abundance and mass must be consistent with the WMAP CMB power spectrum. The lifetime of the X^- also has a lower limit because it must live long enough to allow at least some fraction of the X^- produced initially in the big bang to exist through the epoch of BBN. If the X^- particles decay into leptons and photons at some later stage, they are expected to destroy some fraction of the nuclei to which they had become bound during BBN. However, that fraction is not expected to be large (Kaplinghat & Rajaraman 2006; Rosen 1975) and can be neglected.

2.2. Nuclear Binding Energies

The reaction rates of the X^- nuclei are strongly affected by their binding energies. In our calculations both the binding energies and the eigenstate wave functions of X^- particles were computed by taking into account the modified Coulomb interaction with the nucleus. For this purpose, we assumed that the charge distribution of nuclides is Gaussian. We then solved the two-body Schrödinger equation by a variational calculation (Gaussian expansion method, i.e. Hiyama et al. 2003), and obtained binding energies. The obtained values are listed in Table 1. The adopted root mean square charge radii are listed in the second column. When experimental data exist, we used charge radii determined from experiment. Note that since the X^- particles can bound only electromagnetically to nuclei, their binding energies are typically small ($\sim 0.1 - 1$ MeV), and are largest for heavy nuclei. Hence, they are not appreciably bound to nuclei until the temperature becomes low enough.

2.3. Reaction Rates

The leading term in the expression for the thermonuclear reaction rates (TRR) $\langle\sigma v\rangle$ for nonresonant reactions involving nuclei with embedded X^- particles can be written (e.g. Boyd 2007) as

$$\langle\sigma v\rangle_{\text{NR}} = \left(\frac{2}{\mu}\right)^{1/2} (k_B T) \left(\frac{4}{9}\right) 3^{-1/2} \times E_0^{-3/2} S(E_0) \tau^2 \exp(-\tau), \quad (1)$$

where $E_0 = 1.22(z_1^2 Z_2^2 \mu T_6^2)^{1/3}$ keV is the energy at the peak of the Gamow window, $S(E_0)$ is the "astrophysical S -factor" at E_0 , k_B is the Boltzmann constant, T_6 is the temperature in units of 10^6 K, and

$$\tau = \frac{3E_0}{k_B T} = 42.46 \left(\frac{z_1^2 Z_2^2 \mu}{T_6}\right)^{1/3}. \quad (2)$$

The astrophysical S factor contains the nuclear matrix element for the reaction. For some of the rates we take the nuclear matrix element within $S(E_0)$ to be the same as for the reactions of the corresponding normal nuclei (NACRE; Caughlan & Fowler 1988; Smith et al. 1993). For others we can adopt a scaling relation as described below. Hence, the dominant corrections for the TRR in the above equation arises from the terms involving the reduced mass μ (in atomic mass units), and z_1 and Z_2 (the proton numbers for the projectile normal nucleus and the target X^- -nucleus). We have assumed Z_2 to be the net charge of the bare nucleus and any embedded X^- particles, i.e. $Z_2 = z_2 - n$ for single ($n = 1$) X^- -bound nuclei, where z_2 is the atomic number of the bare nucleus. As noted above, we take the spin of the X^- particles to be zero.

At the epoch during BBN at which the X^- -nuclei undergo nucleosynthesis the neutron abundance is extremely small. Nevertheless, for completeness we have included neutron radiative capture reactions in the reaction network. We adopted the known values for the normal nuclei whenever possible, but those values are not always available for the unstable nuclei of interest $3 \leq z_2 \leq 5$. For the Be_X , $\text{B}_X(n, \gamma)$ reactions we assumed a mean value obtained from the ${}^6\text{Li}(n, \gamma){}^7\text{Li}$ and ${}^7\text{Li}(n, \gamma){}^8\text{Li}$ reactions (see, e.g. Heil et al. 1998; Barker 1980, and references therein) of $40 \mu\text{b}$ at 25 keV.

2.3.1. X^- Transfer Reactions to Produce ${}^6\text{Li}$, ${}^7\text{Li}$ and ${}^7\text{Be}$

Reactions in which an X^- particle can be transferred can be very important in circumventing some of the reactions that would normally be inhibited (Pospelov 2007). This is especially true of the ${}^4\text{He}_X(d, X^-){}^6\text{Li}$ reaction. The rate for this reaction could be orders of magnitude larger than that of the ${}^4\text{He}(d, \gamma){}^6\text{Li}$ reaction. This latter reaction is the main process by which ${}^6\text{Li}$ is made in BBN in the absence of X^- particle. Normally, however, this reaction is suppressed because it is dominated by an electric quadrupole transition.

Hamaguchi et al. (2007) have recently carried out a new theoretical calculation of the cross section for the X^- transfer reaction ${}^4\text{He}_X(d, X^-){}^6\text{Li}$ in the context of a quantum three-body model. Their value was about an order of magnitude smaller than that of Pospelov (2007). This difference can be traced to an exact treatment of the quantum tunneling in the fusion process and the use of a better nuclear potential. We have therefore adopted the

rate of Hamaguchi et al. (2007) as the most reliable estimate for this rate and assume a factor of 3 uncertainty.

Cyburt et al. (2006) estimated astrophysical S -factors for various transfer reactions including the ${}^4\text{He}_X(t, X^-){}^7\text{Li}$, ${}^4\text{He}_X({}^3\text{He}, X^-){}^7\text{Be}$, ${}^6\text{Li}_X(p, X^-){}^7\text{Be}$ reactions by applying a scaling relation (Pospelov 2007),

$$S_X/S_\gamma \propto p_f a_0 / (\omega_\gamma a_0)^{2\lambda+1}, \quad (3)$$

where S_X and S_γ are the S -factors for the X^- transfer and normal radiative processes, respectively. The quantity a_0 is the X^- Bohr radius of ${}^4\text{He}_X$ or ${}^6\text{Li}_X$, while p_f is the linear momentum of the outgoing ${}^7\text{Li}$ or ${}^7\text{Be}$. The quantity ω_γ is the energy of the emitted photon of multipole order λ ($\lambda = 1$ for electric dipole) in the radiative-capture reactions.

In the present work, however, we consider more details of the reaction dynamics in order to better clarify the differences in these reactions. First, we note that ${}^4\text{He}$, ${}^6,{}^7\text{Li}$, and ${}^7\text{Be}$ occupy an s-wave orbit around the X^- particle (assuming the X^- particle to be much heavier than these nuclei). At the same time, the ${}^6\text{Li}$ nucleus is an $\alpha + d$ cluster system in a relative s-wave orbit, while the $A = 7$ nuclei are $\alpha + t$ and $\alpha + {}^3\text{He}$ cluster systems in relative p-wave orbits. This difference in the orbital angular momentum will produce a critical difference in the reaction dynamics between the ${}^4\text{He}_X(d, X^-){}^6\text{Li}$ reaction and the ${}^4\text{He}_X(t, X^-){}^7\text{Li}$, ${}^4\text{He}_X({}^3\text{He}, X^-){}^7\text{Be}$, and ${}^6\text{Li}_X(p, X^-){}^7\text{Be}$ reactions. In particular, the latter three X^- transfer reactions to produce ${}^7\text{Li}$ and ${}^7\text{Be}$ must involve a $\Delta l = 1$ angular momentum transfer. This leads to a large hindrance of the overlap matrix element of the nuclear potential for the X^- transfer processes. In the latter three reactions the outgoing ${}^7\text{Li}$ and ${}^7\text{Be}$ in the final state must occupy a scattering p-wave orbit from the X^- particle in order to conserve total angular momentum. Thus, a realistic quantum mechanical calculation would deduce much smaller S_X -factors than those estimated by Cyburt et al. (2006). In this article, therefore, we have assumed that the above three reaction processes are negligible.

2.3.2. ${}^7\text{Be}_X + p$ Resonant Reaction

Bird et al. (2007) have recently suggested that the ${}^7\text{Be}_X(p, \gamma){}^8\text{B}_X$ resonant reaction could occur through an atomic excited state of ${}^8\text{B}_X$ with a threshold energy of 167 keV. This channel does destroy a significant amount of ${}^7\text{Be}_X$ and is included in our present study.

In the previous study (Kusakabe et al. 2007), we have suggested that a reaction channel through the 1^+ , $E^* = 0.770 \pm 0.010$ MeV nuclear excited state of ${}^8\text{B}$ via ${}^7\text{Be}_X + p \rightarrow {}^8\text{B}^*(1^+, 0.770 \text{ MeV})_X \rightarrow {}^8\text{B}_X + \gamma$ could also destroy ${}^7\text{Be}_X$. However, we found that this channel is unimportant from the estimate of binding energies in this study. In Kusakabe et al. (2007), the binding energies and the eigenstate wave functions of the X -nuclei were calculated assuming uniform finite-size charge distributions of radii $r_0 = 1.2A^{1/3}$ fm for nuclear mass number A (Cahn & Glashow 1981). Since the assumed charge radii were smaller than the measured charge radii, the estimated binding energies were higher than those of this study. Although the nuclear resonance channel is not important, we show the effect of this channel on ${}^7\text{Be}_X$ destruction.

The TRR for resonant radiative capture reactions is given approximately by

$$\langle \sigma v \rangle_R = \hbar^2 \left(\frac{2\pi}{\mu k_B T} \right)^{3/2} \omega_\gamma \exp(-E/k_B T), \quad (4)$$

$$\omega_\gamma = \frac{2I+1}{(2I_1+1)(2I_2+1)} \frac{\Gamma_l \Gamma_\gamma}{\Gamma_{\text{tot}}}, \quad (5)$$

where \hbar is Planck's constant, E is the resonance energy, and I_1 , I_2 , and I are the spins of the projectile, the target, and the resonance. The quantity Γ_l is the particle width for decay into two charged particles of relative angular momentum l , while Γ_γ is the gamma decay width, and Γ_{tot} is the total width of the resonant state.

Γ_l is approximately written (Boyd 2007) as

$$\begin{aligned} \Gamma_l \approx & \frac{3\hbar}{R} \left(\frac{2}{AM_u} \right)^{1/2} \theta_l^2 E_c^{1/2} \\ & \times \exp[bE^{-1/2} + 1.05(ARz_1Z_2)^{1/2} \\ & - 7.62 \left(l + \frac{1}{2} \right)^2 (ARz_1Z_2)^{-1/2}], \end{aligned} \quad (6)$$

where $R = 1.4(A_1^{1/3} + A_2^{1/3}) \times 10^{-13}$ cm is the interaction radius with A_1 and A_2 the atomic weights of the interacting particles. The symbol A denotes the reduced atomic weight $A = A_1 A_2 / (A_1 + A_2)$, and M_u is the atomic mass unit, while θ_l^2 is the dimensionless reduced width. The height of the Coulomb barrier is

$$E_c = 1.44(\text{MeV fm}) \frac{z_1 Z_2}{R}, \quad (7)$$

while the usual Sommerfeld parameter b is given by $b = 31.28z_1Z_2A^{1/2}(\text{keV}^{1/2})$. Correcting the charge, reduced mass, and energy for the nuclides with an embedded X^- particle, we obtain the partial width of the ${}^8\text{B}^*(0.77 \text{ MeV})_X \rightarrow {}^7\text{Be}_X + p$ reaction,

$$\Gamma_{1,X} \approx 1.7 \times 10^6 \text{ eV} \exp\left(-\frac{93.9}{(E_{\text{th}}/\text{keV})^{1/2}}\right), \quad (8)$$

where E_{th} is the energy level of the nuclear resonant state with respect to the ${}^7\text{Be}_X$ plus p exit channel.

From the conjugate analog state of ${}^8\text{Li}$ (1^+ , 0.9809 MeV) we deduce that the ${}^8\text{B}$ (0.770 MeV) first excited state has spin and parity $I^\pi = 1^+$ and that the resonant reaction proceeds through a p-wave ($l = 1$). In Eq. (8) we also adopted $\theta_1^2 = 0.82$ from the TRR of this resonance used in standard BBN. Applying this proton width [Eq. (8)] and $\Gamma_\gamma = 25 \pm 4$ meV (Ajzenberg-Selove 1988) to Eqs. (4) and (5), we can estimate the resonant TRR for ${}^7\text{Be}_X + p \rightarrow {}^8\text{B}^*(1^+, 0.770 \text{ MeV})_X \rightarrow {}^8\text{B}_X + \gamma$ as a function of E . When $E \approx 0$, $\Gamma_{1,X}$ vanishes, thus $\omega_\gamma \rightarrow 0$ and the TRR also vanishes. As the resonance energy E increases, $\Gamma_{1,X}$ also gradually increases and eventually becomes larger than Γ_γ . Thus, ω_γ converges to a constant value $\omega_\gamma = (2I+1)/((2I_1+1)(2I_2+1))\Gamma_\gamma$ in Eq. (5). However, the exponential factor $\exp(-E/k_B T)$ in Eq. (4) strongly regulates the TRR for larger E . In this manner there is a most effective resonance energy E_{eff} which maximizes the TRR. We found $E_{\text{eff}} \approx 30$ keV numerically. Hence, this resonant reaction could be an important, possibly dominant, new means to destroy ${}^7\text{Be}_X$.

The present study, however, indicates that is not the case.

In the previous study (Kusakabe et al. 2007) the calculated binding energies of the X^- particle in ${}^7\text{Be}_X$ and ${}^8\text{B}_X$ were respectively 1.488 MeV and 2.121 MeV. If we adopt these values for the energy levels of the nuclear excited states of ${}^8\text{B}_X$, this 1^+ state of ${}^8\text{B}_X$ becomes located near the particle threshold for the ${}^7\text{Be}_X+p$ channel. In this case the ${}^7\text{Be}_X(p,\gamma){}^8\text{B}_X$ reaction can proceed through a zero-energy resonance of ${}^8\text{B}_X^*$ at $E \approx 0$ MeV, where E is the center-of-mass energy between the ${}^7\text{Be}_X$ and the proton in the entrance channel. We note, however, that the estimated binding energies of X -nuclei, depend upon several assumptions such as the adopted charge distribution of the X^- embedded nucleus (Pospelov 2007; Bird et al. 2007). The $A=6, 7$, and 8 nuclear systems are typical clustering nuclei for which even a small change of the relative wave function between the composite nuclei can affect significantly the radiative capture cross sections at astrophysical energies as well as their static electromagnetic properties (Kajino 1986; Kajino et al. 1988). We therefore adopt a large uncertainty in the 1^+ resonance energy, E , from the ${}^7\text{Be}_X+p$ separation threshold in Kusakabe et al. (2007).

To check the nuclear flow to the higher mass region we added the ${}^8\text{Be}_X+p \rightarrow {}^9\text{B}_X^{*a} \rightarrow {}^9\text{B}_X+\gamma$ reaction, where ${}^9\text{B}_X^{*a}$ indicates that the reaction occurs through an atomic excited state of ${}^9\text{B}$. However this reaction was now found to be unimportant because its threshold energy is relatively large (see Table 2).

2.4. Reaction Network

We show in Fig. 1 the reaction network involving the nuclides with an embedded X^- particle relevant to the present paper. Nuclear reactions denoted by the thick solid arrows were found to be especially important for the production or destruction of the $A=6$ and 7 nuclides both in the literature and in our present study. Pospelov (2007) originally proposed the main production process for ${}^6\text{Li}$ to be the ${}^4\text{He}_X(d,X^-){}^6\text{Li}$ reaction. Similar X^- transfer reactions ${}^4\text{He}_X(t,X^-){}^7\text{Li}$, ${}^4\text{He}_X({}^3\text{He},X^-){}^7\text{Be}$, ${}^6\text{Li}_X(p,X^-){}^7\text{Be}$ were discussed by Cyburt et al. (2006) as possible additional production processes of $A=7$ nuclides. Here we additionally considered the destruction processes ${}^6\text{Li}_X(p,{}^3\text{He}){}^4\text{He}_X$, ${}^7\text{Li}_X(p,\alpha){}^4\text{He}_X$, and ${}^7\text{Be}_X(d,p\alpha){}^4\text{He}_X$. We find, however, that these latter three reactions produce small effect on the BBN results and, as noted above, the latter three X^- transfer reactions would have little effect on BBN results when $\Delta l = 1$ hindrance is taken into account.

Bird et al. (2007) have proposed the likely important destruction process ${}^7\text{Be}_X+p \rightarrow {}^8\text{B}_X^{*a} \rightarrow {}^8\text{B}_X+\gamma$, where ${}^8\text{B}_X^{*a}$ is an atomic excited state through which the radiative capture occurs. They also proposed a charged weak-boson exchange reaction ${}^7\text{Be}_X \rightarrow {}^7\text{Li}+X^0$ followed by ${}^7\text{Li}(p,\alpha){}^4\text{He}$ and ${}^7\text{Li}(X^-,\gamma){}^7\text{Li}_X(p,\alpha){}^4\text{He}_X$ to eventually destroy the $A=7$ nuclides. Other reactions can also contribute to synthesize or destroy ${}^6\text{Li}_{nX}$ and ${}^7\text{Li}_{nX}$, ${}^7\text{Be}_{nX}$ ($n=0$ or 1) and the heavier nuclei. Our network code includes many reactions with nuclei up to Carbon isotopes. Table 2 summarizes our adopted nuclear reaction rates.

2.5. Kinetic Rate Equations

When dealing with the kinetic and chemical equilibrium associated with X^- particles, it is necessary to consider the thermodynamics associated with the binding of X^- particles. This is because it will be important to know precisely when during BBN they become bound to nuclei, and what their distribution over the BBN nuclei is expected to be (Kohri & Takayama 2007). We have put both recombination and ionization processes of X^- particles into our BBN network code and have dynamically solved the associated set of rate equations [as in Kohri & Takayama (2007)] to find when the X -nuclei decoupled from the cosmic expansion. Denoting a specific isotope of an element by (N, Z) , its abundance as $n(N, Z)$, and the corresponding quantities for the isotopes with an embedded X^- as $(N, Z)_X$ and $n(N, Z)_X$, the capture-reionization expressions for (N, Z) and $(N, Z)_X$ in an expanding universe are

$$\begin{aligned} & \frac{\partial n(N, Z)}{\partial t} + 3Hn(N, Z) \\ &= \left[\frac{\partial n(N, Z)}{\partial t} \right]_{\text{creation}} - \left[\frac{\partial n(N, Z)}{\partial t} \right]_{\text{destruction}} \\ & \quad - \left[\frac{\partial n(N, Z)_X}{\partial t} \right]_{\text{capture}}, \end{aligned} \quad (9)$$

and

$$\begin{aligned} & \frac{\partial n(N, Z)_X}{\partial t} + 3Hn(N, Z)_X \\ &= \left[\frac{\partial n(N, Z)_X}{\partial t} \right]_{\text{creation}} - \left[\frac{\partial n(N, Z)_X}{\partial t} \right]_{\text{destruction}} \\ & \quad + \left[\frac{\partial n(N, Z)_X}{\partial t} \right]_{\text{capture}}. \end{aligned} \quad (10)$$

Here, the subscript ‘‘creation’’ refers to nuclear reactions that make (N, Z) and ‘‘destruction’’ to nuclear reactions that destroy it, including β -decay for unstable nuclides. The quantity H is the Hubble expansion rate. Detailed balance of the X -capture reaction $(N, Z) + X^- \rightarrow (N, Z)_X + \gamma$ and its inverse permits (Kohri & Takayama 2007) writing the capture process as

$$\left[\frac{\partial n(N, Z)_X}{\partial t} \right]_{\text{capture}} \approx \langle \sigma_{\text{r}} v \rangle (n_X n(N, Z) - n(N, Z)_X \tilde{n}_\gamma), \quad (11)$$

where σ_{r} is the recombination cross section, n_X is the abundance of X^- particles, and \tilde{n}_γ is the number of photons in excess of E_{bind} , the X^- binding energy to (N, Z) , i.e.,

$$\tilde{n}_\gamma = n_\gamma \left(\frac{\pi^2}{2\zeta(3)} \right) \left(\frac{m_{(N,Z)}}{2\pi T} \right)^{3/2} \exp \left(-\frac{E_{\text{bind}}}{k_B T} \right), \quad (12)$$

and

$$n_\gamma = \left(\frac{2\zeta(3)}{\pi^2} \right) T^3. \quad (13)$$

Note that since E_{bind} is small, the equilibrium will favor unbound X^- particles until low T . Since the mass of the X^- particle is assumed to be $\gtrsim 50$ GeV, the reduced mass for the $X^- + A(N, Z)$ system can be approximated as $\mu_X \equiv m_{A m_X} / (m_A + m_X) \approx m_A$. This leads to

the following TRR for the first recombination process $A(X^-, \gamma)A_X$ (Kohri & Takayama 2007)

$$\begin{aligned} \langle \sigma_r v \rangle_X &\approx \frac{2^9 \pi \alpha Z^2 (2\pi)^{1/2}}{3 \exp(4.0)} \frac{E_{\text{bind}}}{\mu_X^2 (\mu_X T)^{1/2}} \\ &\propto Z^2 E_{\text{bind}} m_A^{-2.5} \sim Z^3 m_A^{-2.5}. \end{aligned} \quad (14)$$

where α is the fine structure constant. This expression is almost independent of m_X but increases with Z . We do, however, obtain a different mass-dependence in the TRR for the second recombination process $A_X(X^-, \gamma)A_{XX}$:

$$\begin{aligned} \langle \sigma_r v \rangle_{XX} &\approx \frac{2^9 \pi \alpha (Z-1)^2 (2\pi)^{1/2}}{3 \exp(4.0)} \frac{E_{\text{bind}}}{\mu_{XX}^2 (\mu_{XX} T)^{1/2}} \\ &\propto (Z-1)^2 E_{\text{bind}} m_X^{-2.5} \sim (Z-1)^3 m_X^{-2.5}. \end{aligned} \quad (15)$$

Here we obtain a mass dependence because $\mu_{XX} \equiv m_{AX} m_X / (m_{AX} + m_X) \approx m_X / 2$. Since m_X is typically much larger than the mass of the light nuclei $m_X \gg m_A$, the rate for the second or higher-order recombination process is hindered.

3. RESULTS

3.1. BBN Calculation Result

Figures 2a and 2b illustrate the results of a BBN calculation in which the X^- abundance is taken to be 10% of the total baryon number, i.e. $Y_X = n_X / n_b = 0.1$, where n_X is the number density of the X^- particles and n_b is the averaged universal baryon-number density. Results shown in Fig. 2a are for normal nuclei while Fig. 2b shows those for the X -nuclei. Note that we adopt the rate of Hamaguchi et al. (2007) for ${}^4\text{He}_X(d, X^-)$, and the reactions ${}^4\text{He}_X(t, X^-)$, ${}^4\text{He}_X({}^3\text{He}, X^-)$, and ${}^6\text{Li}_X(p, X^-)$ are taken to be negligible.

The abundances for the normal nuclei ${}^6\text{Li}$, ${}^7\text{Li}$ and ${}^7\text{Be}$ in the interval $T_9 \sim 0.5 - 0.2$ are seen to be close to their usual BBN values. This is because at higher temperatures the nuclear statistical equilibrium does not particularly favor the production of the weakly bound X -nuclei. Thus, their effect on the abundance is minimal. There are some changes, however, once the X -nuclei appear. Because of the larger binding energies, the X^- particles bind first to the heaviest nuclides, such as ${}^7\text{Li}$ and ${}^7\text{Be}$ produced in normal BBN (first recombination of the X^- particles). These recombinations occur at around $T_9 = 0.3$ (for ${}^7\text{Li}$) and $T_9 = 0.5$ (for ${}^7\text{Be}$), respectively. An increase in the ${}^7\text{Be}_X$ abundance by the recombination can clearly be seen in Fig. 2b. Somewhat later, at around $T_9 = 0.1$, the X^- particles are captured onto ${}^4\text{He}$, as can be seen in Fig. 2b. Then a new round of nucleosynthesis of the X -nuclei, involving the reaction ${}^4\text{He}_X(d, X^-)$, produces normal nuclei ${}^6\text{Li}$ (in Fig. 2a) as well as ${}^6\text{Li}_X$ (in Fig. 2b). However, the most notable feature of these results is that the ${}^6\text{Li}$ is not easily destroyed by the ${}^6\text{Li}(p, \alpha){}^3\text{He}$ reaction, which destroys nearly all of the ${}^6\text{Li}$ produced in standard BBN. This is because the X^- transfer reaction restores the charge of the normal nucleus ${}^6\text{Li}$, which has a Coulomb barrier which is too high at these temperatures for its destruction. Thus, the large abundance ratio of mass 6 to mass 7 is preserved (Pospelov 2007).

In addition, however, ${}^7\text{Be}$ is destroyed by the nuclear reactions that occur after the recombination ($T_9 \sim 0.3$), mainly ${}^7\text{Be}(X^-, \gamma){}^7\text{Be}_X(p, \gamma){}^8\text{B}_X$. This is explained in detail below.

The calculated BBN abundances of the mass 6 and 7 nuclides and other light nuclei depend strongly on the X^- abundance. The above discussion applies only to the case of relatively abundant X^- particles. In order to study the sensitivity of the ${}^6\text{Li}$ and ${}^7\text{Li}$ ($\equiv {}^7\text{Li} + {}^7\text{Be}$) abundances to the X^- abundance, n_X , we carried out a series of BBN calculations in which n_X was varied over a wide range.

Figure 3 shows the calculated abundances of the mass 6 and 7 nuclides. These are plotted as ${}^6\text{Li}/\text{H}$ (solid curves of positive slope) and ${}^7\text{Li}/\text{H}$ (horizontal solid curve), as a function of the initial X^- number fraction f_X relative to the cold dark matter (CDM) abundance, which we define as

$$f_X \equiv \frac{Y_X}{0.09} = \frac{n_X}{n_{\text{CDM}}} \left(\frac{50 \text{ GeV}}{m_{\text{CDM}}} \right). \quad (16)$$

This definition follows if we take number density of CDM particles as that inferred from the CDM closure content ($\Omega_{\text{CDM}} = 0.2$) deduced from the WMAP data. For this closure parameter, the CDM number density, for any value of mass m_{CDM} of the CDM particle, can be written $n_{\text{CDM}} = 0.09 n_b \times (50 \text{ GeV} / m_{\text{CDM}})$. So, our definition of f_X is for a fiducial CDM mass of 50 GeV and is easily scalable to other CDM masses.

In the calculations shown in Fig. 3 we have assumed that the X^- particle has a mean lifetime much longer than the typical time scale for BBN in the presence of X^- particles, i.e. $\tau_X \gg 5$ hours. Below we also consider the case of a mean lifetime which is shorter than 5 hours. In this figure we have taken into account the theoretical uncertainty in the X^- transfer reaction cross sections. For ${}^6\text{Li}$ the upper curves correspond to the yields with our assumed rate for the ${}^4\text{He}_X(d, X^-){}^6\text{Li}$ reaction (Hamaguchi et al. 2007) multiplied by a factor of 3, and the lower curves correspond to that same rate divided by a factor of 3. The middle curve for ${}^6\text{Li}$ corresponds to our best guess for that crucial rate, i.e., the rate of Hamaguchi et al. (2007). As noted above, Bird et al. (2007) suggested that the recombination of ${}^7\text{Be}$ and X^- together with the ${}^7\text{Be}_X(p, \gamma){}^8\text{B}_X$ reaction taking account of the resonant contribution from both reactions would destroy a considerable amount of ${}^7\text{Be}$; this process was included in all of our calculations.

It is clear from Fig. 3 that the ${}^6\text{Li}$ abundance increases monotonically with increasing f_X . This is a consequence of the fact that ${}^6\text{Li}$ is mainly produced by the ${}^4\text{He}_X(d, X^-){}^6\text{Li}$ reaction as proposed in Pospelov (2007) for almost entire range of f_X -values. For $f_X \lesssim 10^{-9}$, however, the standard BBN processes ${}^4\text{He}(d, \gamma){}^6\text{Li}$ and ${}^3\text{He}(t, \gamma){}^6\text{Li}$ are the main reactions to make ${}^6\text{Li}$ (Fukugita & Kajino 1990; Smith et al. 1993). In the region of $f_X \gtrsim 0.1$, however, a departure from the linear increase due to ${}^6\text{Li}(X^-, \gamma){}^6\text{Li}_X(p, {}^3\text{He}){}^4\text{He}_X$ is observed.

During normal BBN, at the baryon to photon ratio deduced from CMB measurement by WMAP, ${}^7\text{Li}$ is produced mainly as ${}^7\text{Be}$. We find that the ${}^7\text{Be}$ (and ${}^7\text{Li}$) produced during the standard BBN epoch captures X^- particles to form ${}^7\text{Be}_X$ (and ${}^7\text{Li}_X$) during the first recombi-

nation. The ${}^7\text{Be}$ is then destroyed by the ${}^7\text{Be}_X(p,\gamma){}^8\text{B}_X$ reaction. In the parameter region of lower X^- abundance $f_X \lesssim 0.1$, ${}^7\text{Be}$ and ${}^7\text{Li}$ are produced in the standard BBN by the ${}^4\text{He}(t,\gamma){}^7\text{Li}$ and ${}^4\text{He}({}^3\text{He},\gamma){}^7\text{Be}$ reactions. They are not, however, destroyed and remain almost unchanged.

3.2. Constraints on the Primordial ${}^6\text{Li}$ Abundance

Constraints on the primordial ${}^6\text{Li}$ abundance must be inferred from the observed plateau as a function of metallicity on MPHSs. The actual primordial abundance of ${}^6\text{Li}$ could be higher than the recently detected high plateau-abundance (Asplund et al. 2006) of ${}^6\text{Li}$ (lower horizontal dashed curve in Fig. 3). This is because stellar processing could have depleted an initial surface abundance. It is expected in models (Pinsonneault et al. 2002) of stellar structure and evolution that both ${}^6\text{Li}$ and ${}^7\text{Li}$ abundances decrease because materials on the stellar surface might be convected to regions of sufficiently high temperature that the fragile ${}^6\text{Li}$ and ${}^7\text{Li}$ are partially destroyed (e.g. Lambert 2004; Richard et al. 2005). Therefore, the plateau level for the observed abundances of ${}^6\text{Li}/\text{H}$ and ${}^7\text{Li}/\text{H}$ in MPHSs should be considered a lower limit to the primordial abundance. For this lower limit we take the 3σ lower limit to the mean plateau value times a factor of $1/3$ for systematic uncertainties giving ${}^6\text{Li}/\text{H} \geq 1.7 \times 10^{-12}$. We include this additional factor because there may be additional systematic uncertainties due to the sensitivity of the inferred ${}^6\text{Li}$ abundance to the model atmosphere employed (Cayrel et al. 2007).

The upper limit is more difficult to estimate. Because ${}^6\text{Li}$ could be more easily destroyed in stars than ${}^7\text{Li}$, its upper limit should be higher than the upper limit to the ${}^7\text{Li}$ abundance. Even so, there are constraints on the degree of stellar processing for both ${}^7\text{Li}$ and ${}^6\text{Li}$ from the limits on the dispersion of the plateau. A large degree of stellar destruction would be sensitive to the varying degrees of meridional circulation in the stars (Pinsonneault et al. 2002) and hence should produce a large dispersion in observed abundances. However, the fact that the observed dispersion in ${}^7\text{Li}$ is greater than that observed for ${}^6\text{Li}$ (albeit on a limited data set) suggests that the destruction may not be very significant (Pinsonneault et al. 2002). For this reason we adopt a conservative upper limit of a factor of 10 above the mean plateau value giving ${}^6\text{Li}/\text{H} \leq 7.1 \times 10^{-11}$.

3.3. Observational Constraints on the X^- Abundance

3.3.1. Case of Longer Mean Life of X^- Decay

We consider several constraints on the X^- abundance from the observed Li isotopic abundances. We first discuss the case of a longer mean life for the X^- particle ($\tau_X \gtrsim 5$ hours). In this case, the yields of BBN are not strongly affected by the value of τ_X . Our adopted lower limit to the ${}^6\text{Li}/\text{H}$ ratio is then satisfied by the calculated abundance of ${}^6\text{Li}/\text{H}$ (thick solid curve in Figs. 3 and 4) for $f_X \gtrsim 2 \times 10^{-6}$.

In order to include the uncertain depletion effect of fragile lithium in stellar atmospheres, we display in Fig. 4 the calculated primordial ${}^6\text{Li}$ and ${}^7\text{Li}$ abundances relative to the mean plateau levels in MPHSs, i.e. $({}^A\text{Li}/\text{H})/({}^A\text{Li}/\text{H})_{\text{MPHS}}$. The gray regions enclose our adopted uncertainty due to the X^- transfer reaction cross sections

as in Fig. 3. Here and below, we take, as our recommended network, the reaction rate of ${}^4\text{He}_X(d,X^-){}^6\text{Li}$ from Hamaguchi et al. (2007).

The parameter regions of initial X^- abundance, $2 \times 10^{-6} \lesssim f_X \lesssim 1 \times 10^{-4}$ for ${}^6\text{Li}$ and $f_X \lesssim 1$ for ${}^7\text{Li}$, respectively, are plausible regions in this context. In addition, since ${}^6\text{Li}$ is more easily destroyed in proton burning than ${}^7\text{Li}$, the primordial abundances should satisfy the inequality $({}^7\text{Li}/\text{H})/({}^7\text{Li}/\text{H})_{\text{MPHS}} \lesssim ({}^6\text{Li}/\text{H})/({}^6\text{Li}/\text{H})_{\text{MPHS}}$. From Fig. 4 we thus find the concordant parameter region of

$$4 \times 10^{-5} \lesssim f_X \lesssim 9 \times 10^{-5},$$

$$\text{(i.e. } 4 \times 10^{-6} \lesssim Y_X \lesssim 8 \times 10^{-6}\text{)}, \quad (17)$$

which is bounded by the vertical solid line on Fig. 4.

Here, we used Eq. (16) to convert the inferred limits on f_X into the limits for Y_X . We then deduce from Eq. (17) and Fig. 4 a possible depletion factor, $d({}^A\text{Li})$, of the primordial abundances of ${}^6\text{Li}$ and ${}^7\text{Li}$ in Population II metal-poor halo stars of,

$$d({}^6\text{Li}) \lesssim 10, \quad (18)$$

$$d({}^7\text{Li}) \lesssim 4, \quad (19)$$

where the upper limit to ${}^6\text{Li}$ depletion comes from our adopted upper limit to the primordial ${}^6\text{Li}$ abundance. We note that these depletion factors are consistent with the known thermonuclear reaction rates for $p+{}^6\text{Li}$ and $p+{}^7\text{Li}$, assuming partial depletion of lithium in the solar atmosphere; the former is about a factor of 80 larger than the latter. We also point out that in our present scenario for BBN including the X^- particles, their abundance parameter region, Eq. (17) can be a solution to the ${}^6\text{Li}$ abundance discrepancy between the standard BBN prediction and the observations of MPHSs, while still satisfying the independent abundance constraint on the primordial ${}^7\text{Li}$ abundance. It is to be noted, however, that there still remains a possible controversy that the depletion factor of $d({}^7\text{Li}) = 3 - 4$ may be too large to accommodate the observed small dispersion in the plateau abundance level detected in MPHSs (Pinsonneault et al. 2002).

3.3.2. Case of Shorter Mean Life of X^- Decay

To study the effects of X^- decay we introduce the lifetime τ_X of the X^- particle. Then there are two parameters Y_X and τ_X . Even in the case when the mean life of the X^- particle is nearly equal to or slightly shorter than five hours ($\tau_X \lesssim 2 \times 10^4$ s) the recombination of ${}^7\text{Be}$ and X^- particles still enriches the ${}^7\text{Be}_X$ abundance (Fig. 2b). This is because the recombination of ${}^7\text{Be}$ and X^- particles occurs at earlier times when the cosmic temperature is $T_9 \sim 0.5$. However, in this case the recombination of ${}^4\text{He}$ cannot produce abundant ${}^4\text{He}_X$. This is because the recombination of ${}^4\text{He}$ occurs at a lower temperature $T_9 \sim 0.1$ when the cosmic time is of the same order of $\tau_X \sim 10^4$ s and is sensitive to the decay. Thus, the ${}^6\text{Li}$ production is reduced because the ${}^4\text{He}_X(d,X^-){}^6\text{Li}$ reaction is strongly hindered.

In this case, however, the resonant reaction process ${}^7\text{Be}_X + p \rightarrow {}^8\text{B}_X^* \rightarrow {}^8\text{B}_X + \gamma$ (Bird et al. 2007) can more effectively destroy ${}^7\text{Be}_X$. We assumed that ${}^8\text{B}_X$ interconverts to ${}^8\text{Be}_X$ by β -decay with a rate of ${}^8\text{B}$ β -decay

multiplied by the correction term $(Q_X/Q)^5$, where Q and Q_X are the Q -values of standard β -decay and that of β -decay for X -nuclei. We adopt here the Hamaguchi et al. (2007) rate for ${}^4\text{He}_X(d, X^-){}^6\text{Li}$.

In Fig. 5, the contours of $d({}^6\text{Li})$ [solid curves] and $d({}^7\text{Li})$ [dashed curves] are shown. The upper and lower solid curves correspond to the abundance level which satisfies our adopted constraint ($1.7 \times 10^{-12} \leq {}^6\text{Li}/\text{H} \leq 7.1 \times 10^{-11}$) as discussed in subsec. 3.2 from the abundance of MPHSs, $({}^6\text{Li}/\text{H})_{\text{MPHS}} = (7.1 \pm 0.7) \times 10^{-12}$ (Asplund et al. 2006). Thus the upper right region of the figure is excluded for ${}^6\text{Li}$ overproduction. The right-upper side from the lower solid curve indicates the region for which the ${}^6\text{Li}$ abundance is higher than that observed in MPHSs.

The three dashed curves correspond to $d({}^7\text{Li})=1.55, 2, 3$, from right to left, respectively. In Fig. 5 there is no ${}^7\text{Li}$ over-destruction region where ${}^7\text{Li}$ abundance is below the observed mean value. $d({}^7\text{Li})=1.55$ corresponds to the 1 sigma upper limit for MPHSs value (Ryan et al. 2000). In the right-upper side from the dashed curve for $d({}^7\text{Li})=2$, the resulting ${}^7\text{Li}$ abundance is lower than ${}^7\text{Li}/\text{H} \approx 2.5 \times 10^{-10}$. Therefore, we conclude that BBN with negatively charged particles provides a simultaneous solution to the ${}^7\text{Li}$ overproduction problem and the ${}^6\text{Li}$ underproduction problem, [as also deduced by Bird et al. (2007)] in the parameter region

$$Y_X \gtrsim 0.9, \quad \tau_X \approx (1.0 - 1.8) \times 10^3 \text{ s}. \quad (20)$$

For $\tau_X \gtrsim 10^5$ s and $Y_X \gtrsim 3$, the calculated abundance of ${}^7\text{Li}$ increases slightly. In this region the ${}^6\text{Li}_X(p, \gamma){}^7\text{Be}_X$ reaction produces some amount of ${}^7\text{Be}_X$. However, this parameter region is uninteresting due to an extreme overproduction of ${}^6\text{Li}$ compared with observed abundances.

In Fig. 5, there is a solid line corresponding to $d({}^6\text{Li})=4$. The condition $({}^7\text{Li}/\text{H})/({}^7\text{Li}/\text{H})_{\text{MPHS}} \lesssim ({}^6\text{Li}/\text{H})/({}^6\text{Li}/\text{H})_{\text{MPHS}}$ or equivalently $d({}^7\text{Li}) \lesssim d({}^6\text{Li})$ is satisfied in the gray region. The gray colored region in Fig. 5 [cf. Eq. (18)] is the most interesting and relevant parameter region in order to solve both the ${}^6\text{Li}$ and ${}^7\text{Li}$ problems. The wider vertical band of $4 \times 10^{-6} \lesssim Y_X \lesssim 8 \times 10^{-6}$ and $\tau_X \gtrsim 10^4$ s corresponds to the solid box bounded by the vertical solid line in Fig. 4 and Eq. (17). This region of the parameter space solves only the ${}^6\text{Li}$ problem, but leaves the ${}^7\text{Li}$ problem unresolved.

Finally, we consider another case where ${}^7\text{Be}_X$ converts to ${}^7\text{Li}$ by a weak charged current transition from X^- to X^0 , i.e. ${}^7\text{Be}_X \rightarrow {}^7\text{Li} + X^0$. This decay quickly transforms ${}^7\text{Be}_X$ to ${}^7\text{Li}$ (type II model in Bird et al. 2007). In this model, the rate of recombination effectively determines the ${}^7\text{Be} \rightarrow {}^7\text{Li}$ conversion rate induced by X^- . The results of this case are shown in Fig. 6. The general features of Fig. 6 are very similar to Fig. 5. However, due to a slightly stronger destruction rate due to the ${}^7\text{Be}_X \rightarrow {}^7\text{Li} + X^0$ decay followed by the ${}^7\text{Li}(p, \alpha){}^4\text{He}$ and ${}^7\text{Li}(X^-, \gamma){}^7\text{Li}_X(p, \alpha){}^4\text{He}_X$ reactions, the contours of the ${}^7\text{Li}$ abundance are systematically shifted toward smaller values of Y_X . The parameter region which solves both the ${}^6\text{Li}$ and ${}^7\text{Li}$ problems also slightly shifts to

$$Y_X \approx 0.04 - 0.2, \quad \tau_X \approx (1.4 - 2.6) \times 10^3 \text{ s}. \quad (21)$$

4. DISCUSSION

4.1. Constraint on Dark Matter Particles

If the dark matter particles, which we denote Y^0 in this article, are the decay products of X^- particles, the cosmological parameter Ω_{CDM} inferred from the WMAP-CMB data can be used to constrain the mass of Y^0 when combined with our abundance constraints on the X^- particles from Eqs. (20) and (21). We suppose that X^- decays to a dark-matter Y^0 particle and any residues, and $Y_Y = Y_X$. The WMAP-CMB constraint on $\Omega_{\text{CDM}} = 0.2$ corresponds to $Y_Y m_Y \lesssim 4.5$ GeV, i.e.

$$Y_X \approx Y_Y \lesssim \frac{4.5 \text{ GeV}}{m_Y}, \quad (22)$$

The calculated abundance constraints on Y_X (Eqs. 20 and 22) can therefore be used to constrain the mass m_Y . Note, that the calculated result in the present study does not particularly depend on the assumed mass of the X^- . In fact, only the second recombination rates and the nuclear reaction rates between X -nuclei depend on the mass of the X^- (see discussion in subsec. 2.5). However, the main production and destruction processes of ${}^6\text{Li}$, ${}^7\text{Li}$, and ${}^7\text{Be}$ are completely free from these processes. We can thus consider the general constraint on the number fraction of X^- particles, Y_X .

The most interesting solution to both the ${}^6\text{Li}$ underproduction and ${}^7\text{Li}$ overproduction involves the parameter space defined in Eqs. (20) and (21). Using [Eq. (20)] in which one includes the destruction reaction process ${}^7\text{Be}_X + p \rightarrow {}^8\text{B}_X^* \rightarrow {}^8\text{B}_X + \gamma$ (Bird et al. 2007), the mass of the dark matter particle Y^0 would be constrained to be

$$m_Y \lesssim 5 \text{ GeV}. \quad (23)$$

However, using [Eq. (21)] in which one includes the ${}^7\text{Be}_X \rightarrow {}^7\text{Li} + X^0$ process (Bird et al. 2007) the allowed mass range increases to

$$m_Y \lesssim 20 - 110 \text{ GeV}, \quad (24)$$

The long lifetime for X^- decay is consistent with the mass of the decaying particle X^- being close to the mass of the daughter particle Y^0 . In this case one can deduce a constraint on the X^- mass of

$$m_X \lesssim O(100 \text{ GeV}). \quad (25)$$

4.2. Initial X^- Abundance at BBN Epoch

Here, we consider a simple estimation of the initial X^- abundance after the BBN epoch taking X^+ and X^- pair annihilation into account. When X^+ and X^- particles are abundant at high temperature, both pair creation and annihilation equilibrate. However, as the universe expands and cools, the annihilation process proceeds until these particles freezeout at some relic X^- (X^+) abundance. A calculation of this is analogous to the well known weakly-interacting massive particle (WIMP) calculation of Kolb & Turner (1990).

Following their derivation, the time evolution the X -to-photon ratio, $\eta_X \equiv n_X/n_\gamma = \eta Y_X$, can be written,

$$\frac{d\eta_X}{dt} = -n_\gamma \langle \sigma v \rangle \eta_X^2. \quad (26)$$

However, unlike the Kolb & Turner (1990) calculation, the X^- annihilation cross section is given by the electromagnetic formation of a positronium-like bound state

(X^-, X^+) system, not by the weak interaction associated WIMPs. Therefore, the annihilation cross section does not scale the same as the WIMP annihilation rate, $\langle\sigma v\rangle_{WIMP} \propto (G_F^2 m_X^2)$, where G_F is the Fermi coupling constant. Rather, the much larger annihilation cross section (Bird et al. 2007) of interest here is given by,

$$\langle\sigma v\rangle = \frac{2^{10}\pi^{3/2}\alpha^3}{3\exp(4)m_X^{3/2}T^{1/2}}. \quad (27)$$

The solution of Eq. (26) is then

$$\eta_X(T) = \left(\frac{1}{\eta_{X_i}} + 2H_i^{-1}n_{\gamma_i}\langle\sigma v\rangle_i \left(1 - \left(\frac{T}{T_i} \right)^{1/2} \right) \right)^{-1}. \quad (28)$$

where the subscript i refers to values at some initial temperature T_i .

Assuming that $\eta_{X_i} \sim O(1)$ and that the baryon-to-photon ratio is $\eta = 6.0 \times 10^{-10}$ (Spergel et al. 2007), the freeze-out abundance of X^- can be written;

$$\begin{aligned} Y_X &\approx \frac{1}{\eta 2H_i^{-1}n_{\gamma_i}\langle\sigma v\rangle_i} \\ &= 0.0057 \left(\frac{g_*}{10.75} \right) \left(\frac{\eta}{6.0 \times 10^{-10}} \right)^{-1} \\ &\quad \times \left(\frac{m_X}{50 \text{ GeV}} \right)^{3/2} \left(\frac{T_i}{50 \text{ GeV}} \right)^{-1/2}, \quad (29) \end{aligned}$$

where g_* is the total number of degrees of freedom of the relativistic particles. This approximation indicates that the charged massive particles that existed in the early universe might remain as relics in abundance of order $Y_X \sim 0.01$. This is not very different from the Y_X -value of the most interesting solution to the ${}^6\text{Li}$ and ${}^7\text{Li}$ problems in Eq. (20) or Eq. (21) which we found, i.e. the solution which leads to the simultaneous destruction of ${}^7\text{Be}$ and production of ${}^6\text{Li}$ at levels that would produce concordance with observations.

4.3. Direct Destruction of Nuclei by X^- Decay

Having shown how primordial X^- particles could result in modified Li isotope production, we need to consider what would happen to those nuclei which retained an embedded X^- particle when the X^- particle decays. This decay was assumed by Kaplinghat & Rajaraman (2006) to interact sufficiently strongly with the host nucleus that it would induce nucleon emission. For example, the decay could knock out a proton or neutron from ${}^4\text{He}_X$, producing either ${}^3\text{He}$ or ${}^3\text{H}$. These nuclides could then interact with other ${}^4\text{He}$ nuclei to produce ${}^6\text{Li}$.

However, this interaction was found by those authors to occur too infrequently, which is consistent with earlier studies (e.g. Rosen 1975). It was therefore concluded that the resulting decay products would have little effect if they were comprised only of leptons and photons. Even so, they might destroy some fraction of the nuclei in which the decays occurred if one of the decay products was a pion (Rosen 1975; Kohri & Takayama 2007). However, for the X^- decays, the decay products might be expected to be electroweakly interacting particles, and the X^- decays might not be expected to significantly affect the host nuclei. We therefore neglect decay-induced destruction in the present study.

4.4. ${}^6\text{Li}$ Production by Electromagnetic Energy Injection from X^- Decay

If the X^- particles decay to charged leptons and any other residues, the high-energy leptons thus produced could interact with background photons to lose their energy and induce additional nonthermal nucleosynthesis. In this section we argue that such nucleosynthesis (if it does occur) does not significantly alter the parameter constraints deduced above.

There is also a viable possibility that the decaying product is an electron. Such a high energy electron quickly interacts with background photons ($e^\pm + \gamma \rightarrow e^\pm + \gamma$ i.e. inverse Compton scattering). The newly produced energetic photons will also interact with background photons ($\gamma + \gamma \rightarrow e^- + e^+$ i.e. pair production). In this way high energy electrons can lose energy by making an electromagnetic cascade shower. Such a shower could trigger non-thermal nucleosynthesis (Dimopoulos et al. 1988a,b, 1989; Jedamzik 2000; Cyburt et al. 2003; Jedamzik 2004; Kawasaki et al. 2005; Kusakabe et al. 2006).

In Kusakabe et al. (2006) the conditions on the parameters of X^- particles which lead to a resolution of the ${}^6\text{Li}$ underproduction problem were delineated. These are $Y_X m_X \geq Y_X E_{\text{EM}} \sim 10^{-4} - 10^{-3}$ GeV and $\tau_X \sim 10^8 - 10^{12}$ s, where E_{EM} is the generated energy in the electromagnetic decay process. The constraint on Y_X for a given X^- mass m_X is then

$$\frac{(10^{-4} - 10^{-3} \text{ GeV})}{m_X} \lesssim Y_X. \quad (30)$$

In the present paper we have considered several destruction processes of ${}^7\text{Be}_X$. Here we note that both Fig. 5 and Fig. 6 indicate the same constraint $Y_X \lesssim 10^{-5}$ from X^- BBN for $\tau_X \sim 10^8 - 10^{12}$ s which is the interesting lifetime range in the previous work based upon electromagnetic X^- decay (Kusakabe et al. 2006). The electromagnetic decay of X^- particles triggers late time ${}^6\text{Li}$ production in amounts of $1 \lesssim d({}^6\text{Li}) \lesssim 10$ for these parameter regions. Therefore, the compatible condition which avoids an overproduction at the earlier epoch and still allows for non-thermal production of ${}^6\text{Li}$ at the later time is only $d({}^6\text{Li}) \lesssim 10$. From this we deduce,

$$\frac{(10^{-4} - 10^{-3} \text{ GeV})}{m_X} \lesssim 1 \times 10^{-5}, \quad (31)$$

which places a lower limit on the mass of the X^- particle of

$$m_X \gtrsim 10 - 100 \text{ GeV}. \quad (32)$$

When m_X satisfies this lower limit, the electromagnetic decay of X^- particles can also operate at times long after the BBN epoch. Clearly, electromagnetic and/or hadronic decays may also contribute to the final computed abundances. And, in a subsequent work we propose to investigate this. However, for now our goal has been to clarify the role of X^- reactions and confirm that this effect alone can explain the observed lithium abundances. Note that in the case where the stable daughter dark matter particle has nearly the same mass as the X^- particle, there is not enough Q -value to produce a hadronic or electromagnetic shower.

5. CONCLUSIONS

We have investigated light-element nucleosynthesis during the big bang in the presence of massive, negatively-charged X^- particles. Such particles would bind to light nuclei in the early universe. As suggested by many authors, they would facilitate BBN by enhancing the nuclear reaction rates both by reducing the charge of the bound X -nuclei, and by enabling transfer reactions involving the X^- particles. We considered the recombination processes of X^- particles and normal nuclei. Our conclusions are as follows:

First, as suggested in previous studies, the X^- particles greatly enhance the production of ${}^6\text{Li}$. The main production process of ${}^6\text{Li}$ is the sequence of ${}^4\text{He}_X$ production through X^- capture on ${}^4\text{He}$ followed by the X^- transfer reaction ${}^4\text{He}_X(d, X^-){}^6\text{Li}$. The resultant ${}^7\text{Li}$ abundance, however is almost the same as normal BBN value unless there is a large X^- abundance $Y_X \gtrsim 0.1$.

Secondly, when the lifetime of the X^- particle is much longer than the period of normal BBN, the ${}^6\text{Li}$ abundance monotonically increases with the X^- particle abundance, except for very small X^- abundance ($Y_X \lesssim 10^{-10}$). On the other hand, the ${}^7\text{Li}$ abundance is nearly independent of the X^- particle abundance unless the X^- particle abundance is larger than ~ 0.1 times the total abundance of baryons. In this case the ${}^7\text{Li}$ abundance decreases with the X^- particle abundance due to the resonance reaction of ${}^7\text{Be}_X(p, \gamma){}^8\text{B}_X$ which reduces the ${}^7\text{Li}$ abundance.

Thirdly, the ${}^6\text{Li}/\text{H}$ and ${}^7\text{Li}/\text{H}$ observed in MPHSSs can constrain the lifetime and abundance of an X^- particle. These observational constraints require the lifetime and abundance to be in the ranges of $\tau_X \approx (1.0 - 1.8) \times 10^3$ s and $Y_X \gtrsim 0.9$. When the reaction ${}^7\text{Be}_X \rightarrow {}^7\text{Li} + X^0$ is also taken into account, these ranges change to $\tau_X \approx (1.4 - 2.6) \times 10^3$ s and $Y_X \approx 0.04 - 0.2$. Therefore, introducing X^- particles with an adequate lifetime and abundance can be a solution for both of the factor of ~ 1000 underproduction of ${}^6\text{Li}$ and the factor of 3-4 overproduction of ${}^7\text{Li}$ in standard BBN.

Fourthly, a constraint on the X^- particle mass can be made from the dark-matter content deduced from the WMAP analysis of the CMB. If the abundance of X^- particles is $Y_X \gtrsim 0.1 - 1$ as summarized above,

the mass of dark matter particles Y^0 , which are produced from the decay of X^- particles, turns out to be $m_Y \lesssim 10 - 100$ GeV, thus leading to the constraint $m_X \lesssim O(100 \text{ GeV})$ when $m_X \sim m_Y$.

In summary, although several possible solutions have been proposed to solve the underproduction problem of ${}^6\text{Li}$, they do not necessarily resolve the overproduction problem of ${}^7\text{Li}$ simultaneously. Pospelov (2007) and Cyburt et al. (2006) proposed the X^- transfer reactions to produce ${}^6\text{Li}$ and ${}^7\text{Li}$. Regarding ${}^6\text{Li}$ production, however, Hamaguchi et al. (2007) have shown that the assumed reaction cross section is not as large as the value deduced by Pospelov. Bird et al. (2007) proposed new destruction processes of ${}^7\text{Be}_X$ through atomic excitations, and we here investigated yet another destruction process through a ${}^8\text{B}_X^*$ nuclear excited resonance in order to resolve the ${}^7\text{Li}$ overproduction problem. The destruction efficiency of these newly proposed processes depends on the excitation energies above the $p+{}^7\text{Be}_X$ separation threshold. We then found that a better estimation of the binding energies leads to negligible effect from the nuclear excited resonance. It would be useful, however, in future work to predict more precisely the binding energies and excited states of exotic X -nuclei and their reaction cross sections utilizing a more realistic quantum mechanical treatment.

We are very grateful to Professor Masayasu Kamimura for enlightening suggestions on the nuclear reaction rates for transfer and radiative capture reactions. This work has been supported in part by the Mitsubishi Foundation, the Grant-in-Aid for Scientific Research (17540275) of the Ministry of Education, Science, Sports and Culture of Japan, and the JSPS Core-to-Core Program, International Research Network for Exotic Femto Systems (EFES). MK acknowledges the support by the Japan Society for the Promotion of Science. Work at the University of Notre Dame was supported by the U.S. Department of Energy under Nuclear Theory Grant DE-FG02-95-ER40934. RNB gratefully acknowledges the support of the National Astronomical Observatory of Japan during his stay there.

REFERENCES

- Ajzenberg-Selove, F. 1988, Nuclear Physics A, 490, 1
 Asplund, M., Lambert, D. L., Nissen, P. E., Primas, F., & Smith, V. V. 2006, ApJ, 644, 229
 Barker, F. C. 1980, Australian Journal of Physics, 33, 159
 Bird, C., Koopmans, K., & Pospelov, M. 2007, ArXiv High Energy Physics - Phenomenology e-prints, arXiv:hep-ph/0703096
 Boyd, R. N. 2007, Introduction to Nuclear Astrophysics (Chicago: University of Chicago Press)
 Cahn, R. N., & Glashow, S. L. 1981, Science, 213, 607
 Caughlan, G. R., & Fowler, W. A. 1988, Atomic Data and Nuclear Data Tables, 40, 283
 Cayrel, R., et al. 2007, A&A, 473, L37
 Cyburt, R. H., Ellis, J., Fields, B. D., & Olive, K. A. 2003, Phys. Rev. D, 67, 103521
 Cyburt, R. H., Ellis, J., Fields, B. D., Olive, K. A., & Spanos, V. C. 2006, Journal of Cosmology and Astro-Particle Physics, 11, 14
 Dimopoulos, S., Esmailzadeh, R., Starkman, G. D., & Hall, L. J. 1988, Physical Review Letters, 60, 7
 Dimopoulos, S., Esmailzadeh, R., Starkman, G. D., & Hall, L. J. 1988, ApJ, 330, 545
 Dimopoulos, S., Esmailzadeh, R., Hall, L. J., & Starkman, G. D. 1989, Nuclear Physics B, 311, 699
 Feng, J. L. et al. (2003a) PRL, 92, 011302
 Feng, J. L. et al. (2003b) PRD, 68, 063504
 Fowler, W. A., Caughlan, G. R., & Zimmerman, B. A. 1967, ARA&A, 5, 525
 Fukuda, M., et al. 1999, Nuclear Physics A, 656, 209
 Fukugita, M., & Kajino, T. 1990, Phys. Rev. D, 42, 4251
 Hamaguchi, K., Hatsuda, T., Kamimura, M., Kino, Y., & Yanagida, T. T. 2007, Physics Letters B, 650, 268
 Hiyama, E., Kino, Y., & Kamimura, M. 2003, Progress in Particle and Nuclear Physics, 51, 223
 Jedamzik, K. 2000, Physical Review Letters, 84, 3248
 Jedamzik, K. 2004, Phys. Rev. D, 70, 063524
 Jedamzik, K. 2008a, Phys. Rev. D, 77, 063524
 Jedamzik, K. 2008b, Journal of Cosmology and Astro-Particle Physics, 0803, 008
 Heil, M., K appeler, F., Wiescher, M., & Mengoni, A. 1998, ApJ, 507, 997
 Kajino, T. 1986, Nuclear Physics A, 460, 559

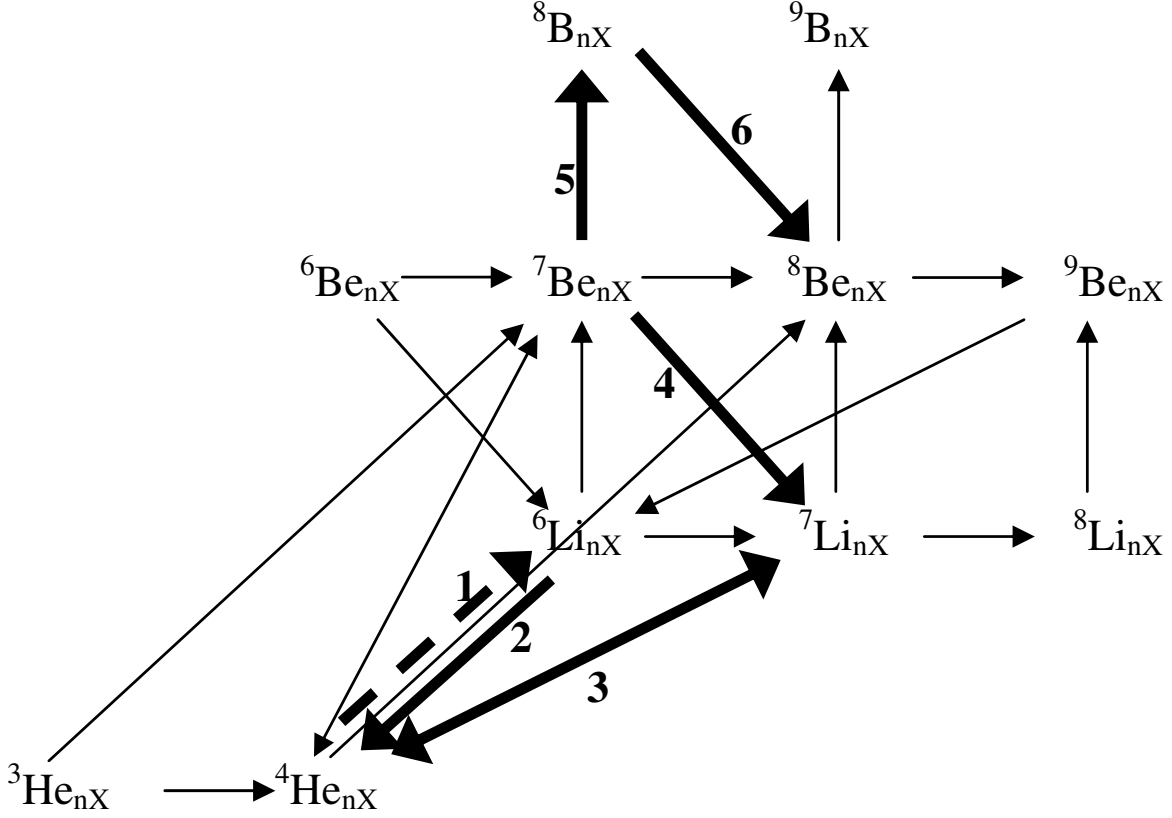


FIG. 1.— Reaction pathways (solid arrows along the directions of positive Q -values) that ultimately occur for the nuclides with an embedded X^- particle. The integer “ n ” can be 0 or 1. Thick solid arrows indicate the most important reactions which contribute to synthesizing or destroying ${}^6\text{Li}_X$, ${}^7\text{Li}_X$, and ${}^7\text{Be}_X$. A thick dashed arrow indicates the X^- transfer reaction ${}^4\text{He}_X(d, X^-){}^6\text{Li}$. Numbers attached indicate: 1. ${}^4\text{He}_X(d, X^-){}^6\text{Li}$; 2. ${}^6\text{Li}_X(p, {}^3\text{He}){}^4\text{He}_X$; 3. ${}^4\text{He}_X(t, \gamma){}^7\text{Li}_X$ & ${}^7\text{Li}_X(p, \alpha){}^4\text{He}_X$; 4. ${}^7\text{Be}_X(X^0){}^7\text{Li}$; 5. ${}^7\text{Be}_X(p, \gamma){}^8\text{B}_X$; 6. ${}^8\text{B}_X(e^+\nu_e){}^8\text{Be}_X$

- Kajino, T., Toki, H., Kubo, K.-I., & Tanihata, I. 1988, *Physics Letters B*, 202, 475
- Kaplinghat, M., & Rajaraman, A. 2006, *Phys. Rev. D*, 74, 103004
- Kawano, L. 1992, NASA STI/Recon Technical Report N, 92, 25163
- Kawasaki, M., Kohri, K., & Moroi, T. 2005, *Phys. Rev. D*, 71, 083502
- Kohri, K., & Takayama, F. 2007, *Phys. Rev. D*, 76, 063507
- Kolb, E. W., & Turner, M. S. 1990, *The Early Universe*, *Frontiers in Physics*, 69 (California: Addison-Wesley)
- Kusakabe, M., Kajino, T., & Mathews, G. J. 2006, *Phys. Rev. D*, 74, 023526
- Kusakabe, M. 2007, *ApJ*, submitted
- Kusakabe, M., Kajino, T., Boyd, R. N., Yoshida, T., & Mathews, G. J. 2007, *Phys. Rev. D*, in press
- Lambert, D. L. 2004, *The New Cosmology: Conference on Strings and Cosmology*, 743, 206
- Meléndez, J., & Ramírez, I. 2004, *ApJ*, 615, L33
- Pinsonneault, M. H., Steigman, G., Walker, T. P., & Narayanan, V. K. 2002, *ApJ*, 574, 398
- Pospelov, M. 2007, *Physical Review Letters*, 98, 231301
- Prantzos, N. 2006, *A&A*, 448, 665
- Richard, O., Michaud, G., & Richer, J. 2005, *ApJ*, 619, 538
- Rollinde, E., Vangioni, E., & Olive, K. A. 2006, *ApJ*, 651, 658
- Rosen, S. P. 1975, *Physical Review Letters*, 34, 774
- Ryan, S. G., Beers, T. C., Olive, K. A., Fields, B. D., & Norris, J. E. 2000, *ApJ*, 530, L57
- Sigurdson, K. & Kamionkowski, M. (2004) *Phys. Rev. Lett.*, 92, 171302
- Simon, G. G., Schmitt, C., & Walther, V. H. 1981, *Nuclear Physics A*, 364, 285
- Smith, M. S., Kawano, L. H., & Malaney, R. A. 1993, *ApJS*, 85, 219
- Spiegel, D. N., et al. 2007, *ApJS*, 170, 377
- Tanihata, I., Kobayashi, T., Yamakawa, O., Shimoura, S., Ekuni, K., Sugimoto, K., Takahashi, N., Shimoda, T., & Sato, H. 1988, *Physics Letters B*, 106, 592
- Yao, W.-M., & et al. 2006, *Journal of Physics G Nuclear Physics*, 33, 1

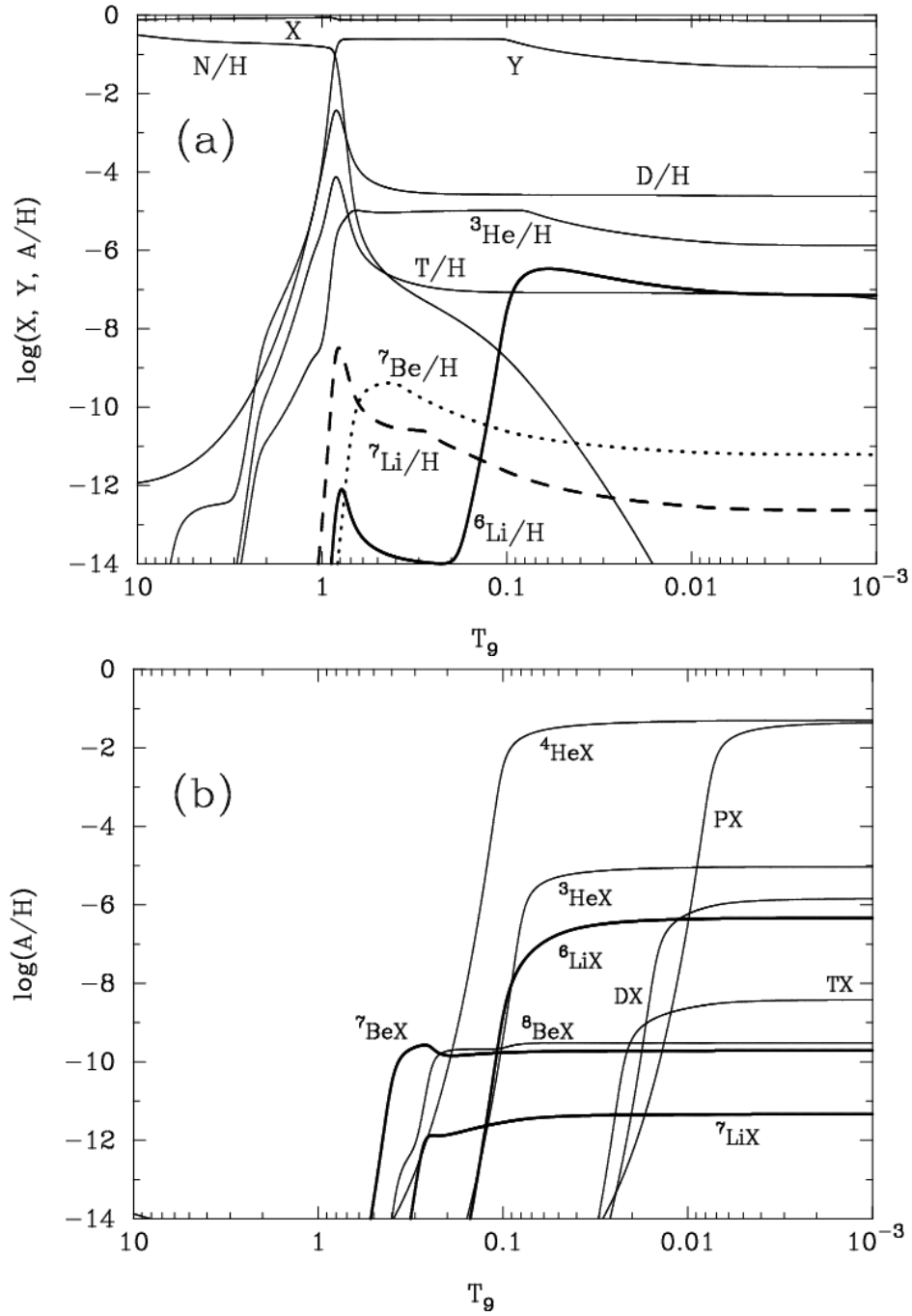


FIG. 2.— Calculated abundances of normal nuclei (a) and X -nuclei (b) as a function of T_9 . For this figure we have taken the abundance of negatively charged particles X^- to be $Y_X = n_X/n_b = 0.1$, and its lifetime is taken to be long $\tau_X = \infty$. We utilize the X^- reaction rates as described in the text.

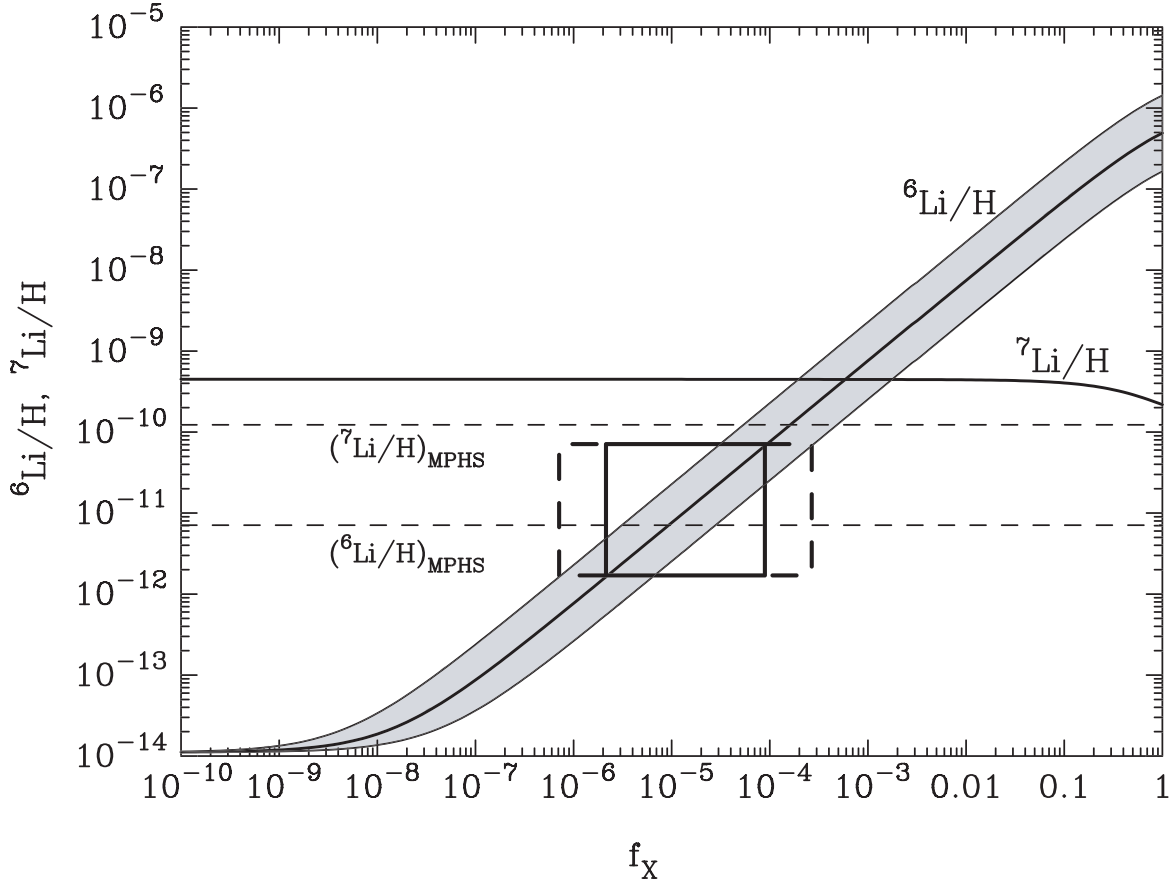


FIG. 3.— Calculated abundances of ${}^6\text{Li}/\text{H}$ and ${}^7\text{Li}/\text{H}$ as a function of the initial X^- abundance parameter f_X defined in the text. The gray band bounded by curves of ${}^6\text{Li}$ show the uncertainty from the rate for X^- transfer reaction. The dashed lines indicate the mean values observed in MPHSs. The dashed and solid boxes indicate the range of f_X consistent with our adopted limits on the abundance of ${}^6\text{Li}/\text{H}$ observed in MPHSs.

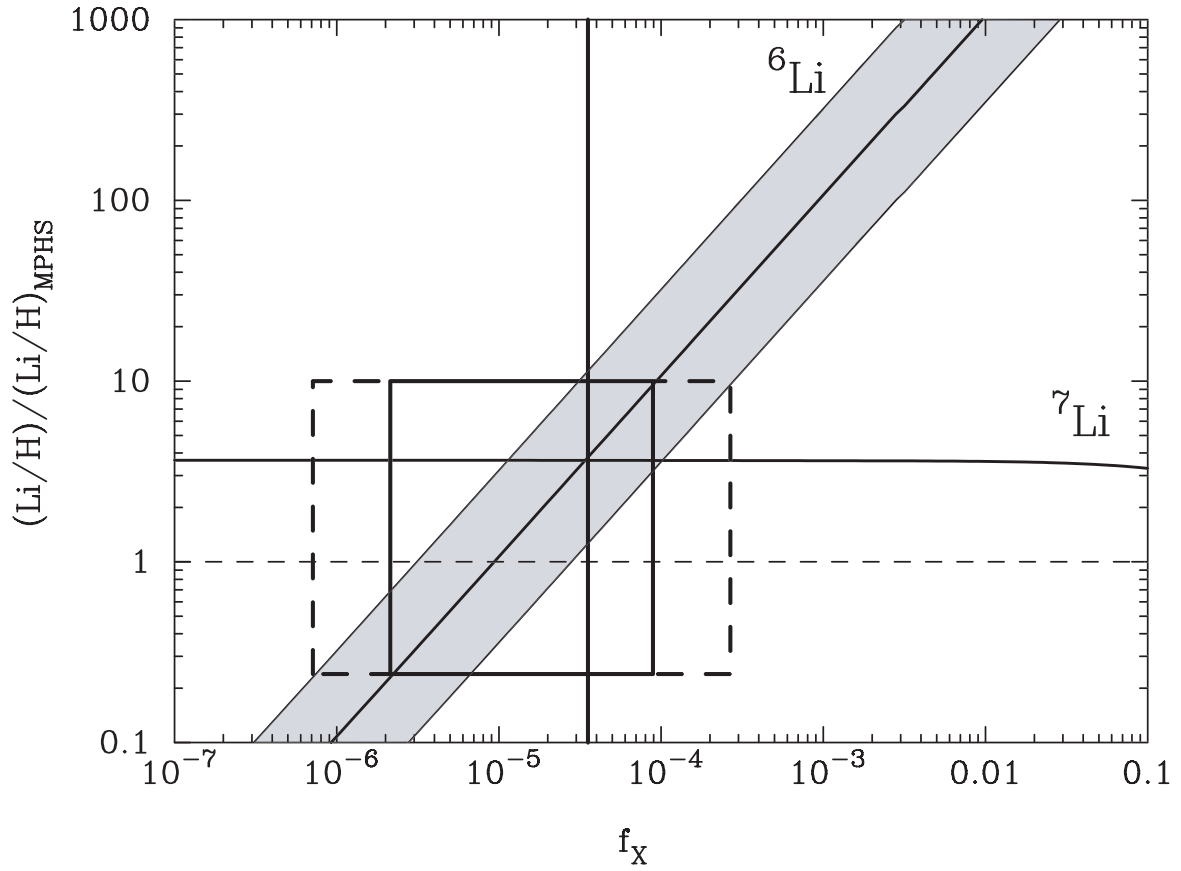


FIG. 4.— Calculated abundances of ${}^6\text{Li}/\text{H}$ and ${}^7\text{Li}/\text{H}$ normalized to the mean value observed in MPHSs as a function of f_X . The solid (dashed) boxes are similar to those of Fig. 3. The vertical solid line corresponds to the lowest abundance of X^- (f_X) which leads to a larger enhancement of ${}^6\text{Li}$ than ${}^7\text{Li}$.

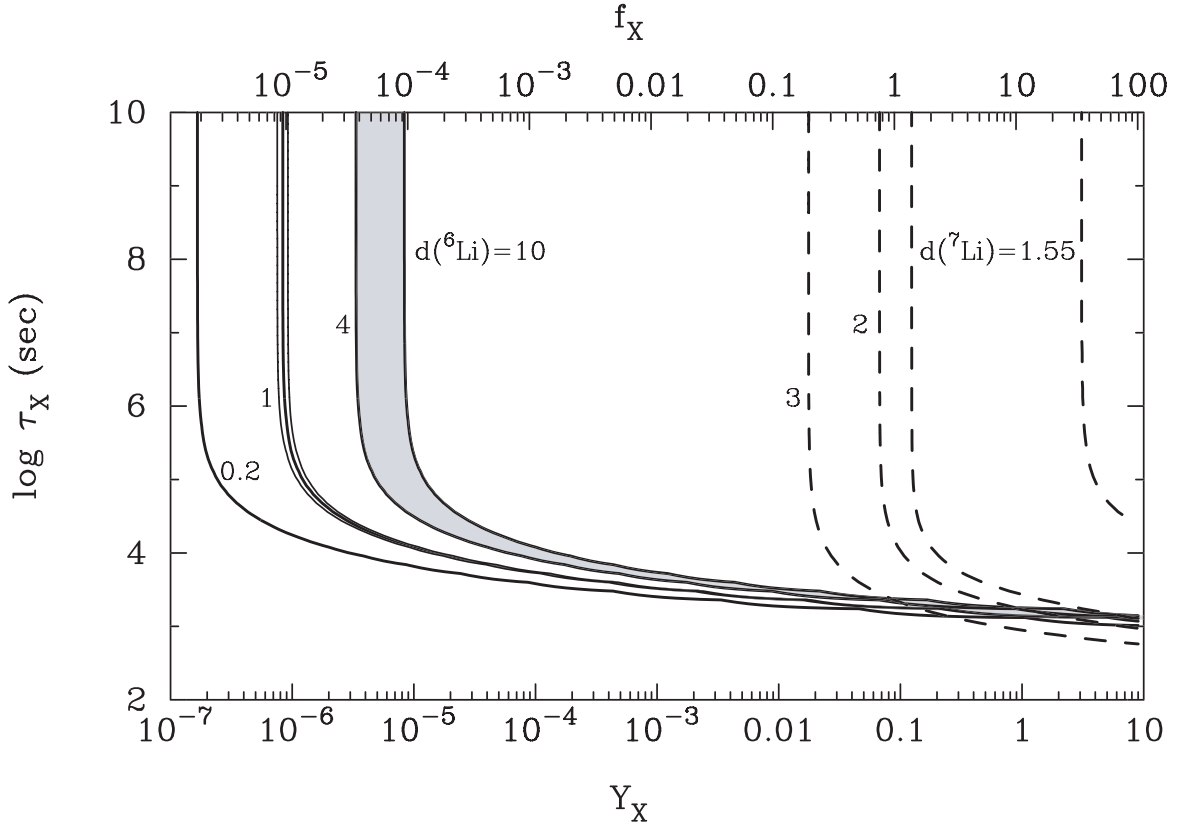


FIG. 5.— Contours of constant lithium abundance relative to the value observed in MPHSs, i.e., $d(^6\text{Li}) = ^6\text{Li}^{\text{Calc}}/{}^6\text{Li}^{\text{Obs}}$ (solid curves) and $d(^7\text{Li}) = ^7\text{Li}^{\text{Calc}}/{}^7\text{Li}^{\text{Obs}}$ (dashed curves). The adopted abundances are ${}^7\text{Li}/\text{H} = (1.23^{+0.68}_{-0.32}) \times 10^{-10}$ (Ryan et al. 2000) and ${}^6\text{Li}/\text{H} = (7.1 \pm 0.7) \times 10^{-12}$ (Asplund et al. 2006). Thin solid lines around the lines of $d(^6\text{Li}) = 1$ curve enclose the 1σ uncertainty in the adopted observational constraint based upon the dispersion of the observed plateau. In the gray region, the condition $d(^6\text{Li}) > d(^7\text{Li})$ is satisfied.

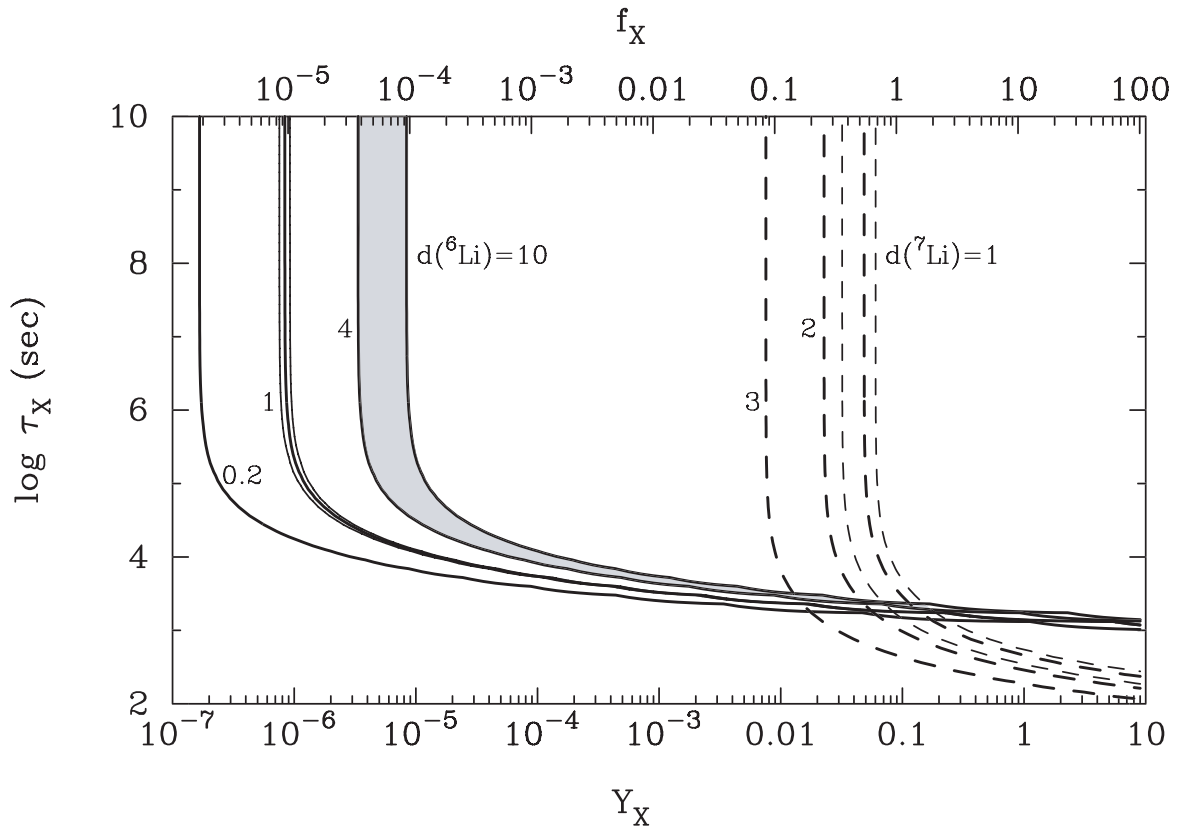


FIG. 6.— Same as in Fig. 5 when the charged-current decay of ${}^7\text{Be}_X \rightarrow {}^7\text{Li} + X^0$ is included. Thin dashed lines around the lines of $d(^7\text{Li}) = 1$ curve enclose the 1σ uncertainty in the adopted observational constraint based upon the dispersion of the observed plateau.

TABLE 1
 BINDING ENERGIES OF X^- PARTICLES TO NUCLEI

nuclide	r_c^{RMS} (fm) ^a	References	E_{Bind} (MeV)
$^1\text{H}_X$	0.875 ± 0.007	1	0.025
$^2\text{H}_X$	2.116 ± 0.006	2	0.049
$^3\text{H}_X$	1.755 ± 0.086	3	0.072
$^3\text{He}_X$	1.959 ± 0.030	3	0.268
$^4\text{He}_X$	1.80 ± 0.04	4	0.343
$^6\text{Li}_X$	2.48 ± 0.03	4	0.806
$^7\text{Li}_X$	2.43 ± 0.02	4	0.882
$^8\text{Li}_X$	2.42 ± 0.02	4	0.945
$^6\text{Be}_X$	$2.52 \pm 0.02^{\text{b}}$	4	1.234
$^7\text{Be}_X$	2.52 ± 0.02	4	1.324
$^8\text{Be}_X$	$2.52 \pm 0.02^{\text{b}}$	4	1.401
$^9\text{Be}_X$	2.50 ± 0.01	4	1.477
$^7\text{B}_X$	$2.68 \pm 0.12^{\text{c}}$	5	1.752
$^8\text{B}_X$	2.68 ± 0.12	5	1.840
$^9\text{B}_X$	$2.68 \pm 0.12^{\text{c}}$	5	1.917

NOTE. — References: 1= Yao & et al. (2006);
 2= Simon et al. (1981); 3=TUNL Nuclear
 Data, <http://www.tunl.duke.edu/NuclData>; 4=
 Tanihata et al. (1988); 5= Fukuda et al. (1999).

^a Root mean square charge radius

^b Taken from ^7Be radius

^c Taken from ^8B radius

TABLE 2
NUCLEAR REACTION RATES OF X -NUCLIDES

Reaction	Reaction Rate (cm ³ s ⁻¹ mole ⁻¹)	Reverse Coefficient ^a	Q (MeV)
³ He _X (n,γ) ⁴ He _X	7.2	3.95	20.653
³ He _X (d,p) ⁴ He _X	$3.9 \times 10^{10} T_9^{-2/3} \exp(-5.36/T_9^{1/3})$	8.49	18.428
⁶ Li _X (n,γ) ⁷ Li _X	5.2×10^3	1.48	7.327
⁶ Li _X (n,t) ⁴ He _X	1.7×10^8	0.577	4.321
⁶ Li _X (p,γ) ⁷ Be _X	$5.5 \times 10^5 T_9^{-2/3} \exp(-6.74/T_9^{1/3})$	1.48	6.124
⁶ Li _X ($p,^3\text{He}$) ⁴ He _X	$2.7 \times 10^{10} T_9^{-2/3} \exp(-6.74/T_9^{1/3})$	0.577	3.557
⁷ Li _X (n,γ) ⁸ Li _X	5.2×10^3	1.58	2.096
⁷ Li _X (p,γ) ⁸ Be _X	$1.3 \times 10^5 T_9^{-2/3} \exp(-6.74/T_9^{1/3})$	7.89	17.774
⁷ Li _X (p,α) ⁴ He _X	$9.0 \times 10^8 T_9^{-2/3} \exp(-6.74/T_9^{1/3})$	1.00	16.808
⁸ Li _X (p,γ) ⁹ Be _X	$1.0 \times 10^5 T_9^{-2/3} \exp(-4.25/T_9^{1/3})$	2.47	17.420
⁶ Be _X (n,γ) ⁷ Be _X	5.2×10^3	0.493	10.766
⁶ Be _X (n,p) ⁶ Li _X	2.7×10^9	0.333	4.642
⁷ Be _X (n,γ) ⁸ Be _X	5.2×10^3	7.89	18.977
⁷ Be _X (n,p) ⁷ Li _X	2.7×10^9	1.00	1.202
⁷ Be _X (p,γ) ⁸ B _X	$1.6 \times 10^8 T_9^{-2/3} \exp(-8.86/T_9^{1/3})$ $+1.6 \times 10^6 T_9^{-3/2} \exp(-1.92/T_9)$	1.58	0.654
⁷ Be _X (d,p) ⁸ Be _X	$8.9 \times 10^{11} T_9^{-2/3} \exp(-11.13/T_9^{1/3})$	16.97	16.752
⁷ Be _X ($d,p\alpha$) ⁴ He _X	$8.9 \times 10^{11} T_9^{-2/3} \exp(-11.13/T_9^{1/3})$	2.15	15.786
⁸ Be _X (n,γ) ⁹ Be _X	5.2×10^3	2.47	1.741
⁸ Be _X (p,γ) ⁹ B _X	$1.4 \times 10^6 T_9^{-3/2} \exp(-5.60/T_9)$	2.47	0.331
⁹ Be _X (n,γ) ¹⁰ Be _X	5.2×10^3	7.89	6.913
⁹ Be _X (p,γ) ¹⁰ B _X	$1.2 \times 10^7 T_9^{-2/3} \exp(-8.83/T_9^{1/3})$	1.13	7.145
¹⁰ Be _X (p,γ) ¹¹ B _X	$1.2 \times 10^7 T_9^{-2/3} \exp(-8.83/T_9^{1/3})$	0.493	11.750
⁹ B _X (n,γ) ¹⁰ B _X	5.2×10^3	1.13	8.556
⁹ B _X (p,γ) ¹⁰ C _X	$1.9 \times 10^5 T_9^{-2/3} \exp(-10.70/T_9^{1/3})$	7.89	4.727
¹⁰ B _X (n,γ) ¹¹ B _X	5.2×10^3	3.45	11.517
¹⁰ B _X (p,γ) ¹¹ C _X	$1.9 \times 10^5 T_9^{-2/3} \exp(-10.70/T_9^{1/3})$	3.45	9.366
¹¹ B _X (p,γ) ¹² C _X	$1.9 \times 10^7 T_9^{-2/3} \exp(-10.70/T_9^{1/3})$	7.89	16.638
¹⁰ C _X (n,γ) ¹¹ C _X	5.2×10^3	0.493	13.195
¹¹ C _X (n,γ) ¹² C _X	5.2×10^3	7.89	18.789
⁴ He _X (d,γ) ⁶ Li _X	$2.2 \times 10^1 T_9^{-2/3} \exp(-5.35/T_9^{1/3})$	2.79	1.936
³ He _X (α,γ) ⁷ Be _X	$2.9 \times 10^6 T_9^{-2/3} \exp(-10.70/T_9^{1/3})$	3.95	2.642
⁴ He _X (t,γ) ⁷ Li _X	$2.0 \times 10^5 T_9^{-2/3} \exp(-6.12/T_9^{1/3})$	2.56	3.006
⁴ He _X (³ He, γ) ⁷ Be _X	$3.2 \times 10^6 T_9^{-2/3} \exp(-9.72/T_9^{1/3})$	2.56	2.567
⁴ He _X (⁶ Li, γ) ¹⁰ B _X	$2.4 \times 10^6 T_9^{-2/3} \exp(-16.05/T_9^{1/3})$	6.22	6.154
⁹ Be _X ($p,^6\text{Li}$) ⁴ He _X	$1.9 \times 10^{11} T_9^{-2/3} \exp(-8.83/T_9^{1/3})$	0.181	0.991
⁴ He _X (α,γ) ⁸ Be _X	$2.9 \times 10^6 T_9^{-2/3} \exp(-10.70/T_9^{1/3})^b$	7.89	0.966
⁶ Li _X (α,γ) ¹⁰ B _X	$3.0 \times 10^6 T_9^{-2/3} \exp(-16.98/T_9^{1/3})$	3.38	5.692
⁷ Li _X (α,γ) ¹¹ B _X	$2.7 \times 10^7 T_9^{-2/3} \exp(-16.98/T_9^{1/3})$	7.89	9.882
⁷ Be _X (α,γ) ¹¹ C _X	$6.6 \times 10^7 T_9^{-2/3} \exp(-22.26/T_9^{1/3})$	7.89	8.934
⁴ He _X (d,X^-) ⁶ Li	$2.37 \times 10^8 (1 - 0.34T_9) T_9^{-2/3} \exp(-5.33/T_9^{1/3})$	0.192	1.131
⁶ Be _X ($e^+\nu_e$) ⁶ Li _X	$T_{1/2} = 2.3$ s		3.349
⁸ B _X ($e^+\nu_e$) ⁸ Be _X	$T_{1/2} = 1.2$ s		17.030

^a For nuclides $a = i, j, k, \dots$ with mass numbers A_a and spins g_a , the reverse coefficients are defined as follows (Fowler et al. 1967) on the assumption that X^- particle is much heavier than nuclides: $0.9867(g_i g_j / g_k) A_j^{3/2}$ for a process $i_X(j, \gamma) k_X$, $(g_i g_j / (g_k g_l)) (A_j / A_k)^{3/2}$ for a process $i_X(j, k) l_X$, and $1.0134(g_i g_j / (g_k g_l g_m)) (A_j / (A_k A_l))^{3/2}$ for a process $i_X(j, kl) m_X$.

^b The S -factor for the reaction ³He(α, γ)⁷Be was used